Pushing Forward Jet Substructure Measurements in Heavy-Ion Collisions

Daniel Pablos

in collaboration with A. Soto-Ontoso

Fellini
Fellowship for Innovation at INFN

INFN
Istituto Nazionale di Fisica Nucleare

This project has received funding from the European Union's Horizon 2020 research and innovation programme under the Marie Skłodowska-Curie grant agreement n. 754496.

Hard Probes 2023
Aschaffenburg, 29th March 2023

Narrowing of Jet Substructure

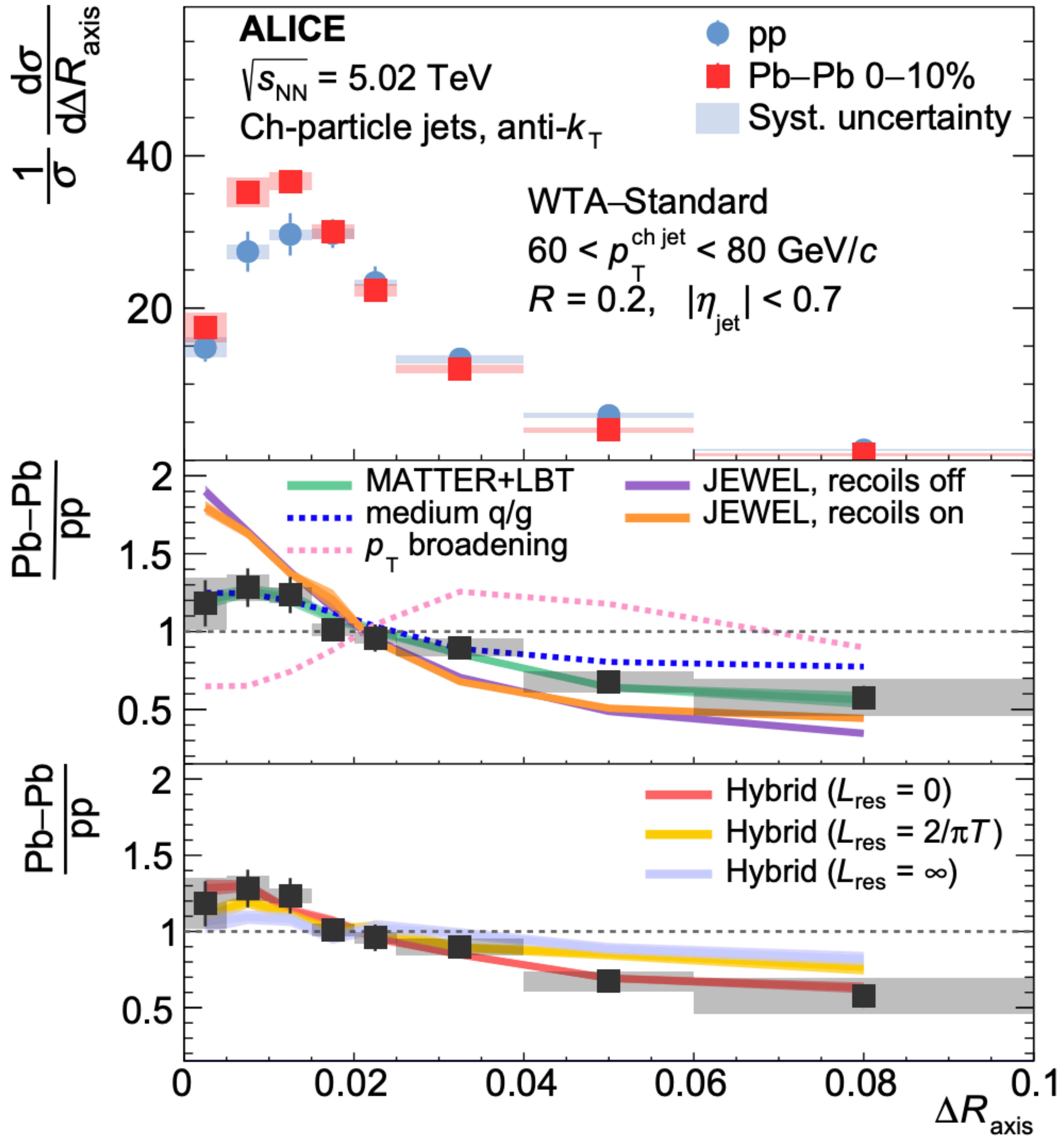

ALICE, 2303.13347

Rey's talk on Tue

Example: WTA axis distance w.r.t. anti-k_T axis

Many Monte Carlo models get similar results.

Bias towards narrower, less active jets.

Medium q/g can also account for the signal.

Strong suppression of gluon jets (factor 4 w.r.t. pp).

Qiu et al. - PRL '19

Medium q/g + p_T broadening fails.

Not accounting for selection bias, while broadening emissions, results in a broader jet ensemble.

Ringer et al. - PLB '19

Jets and Jets

Wide jet

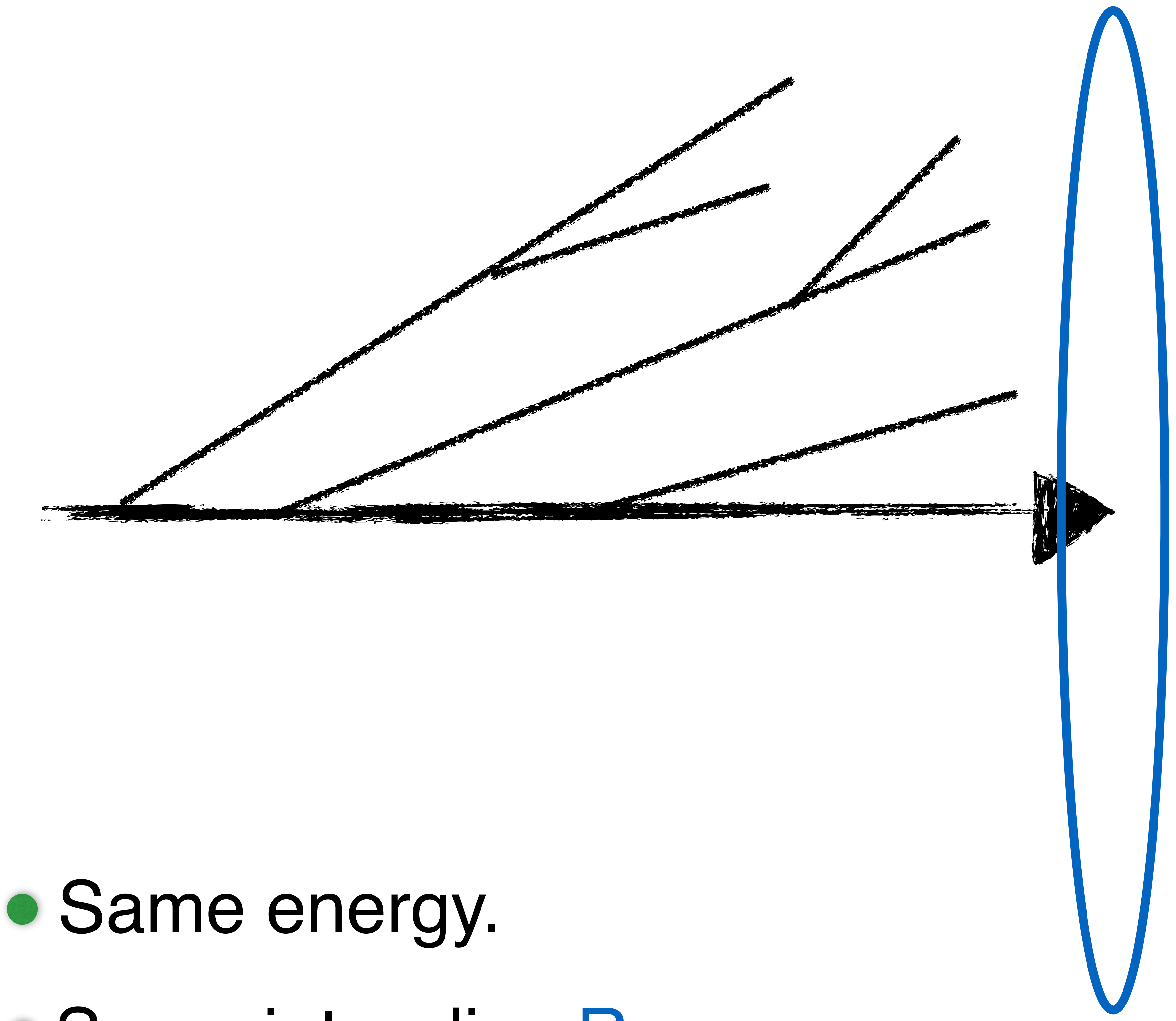

Vacuum-like emission

Narrow jet

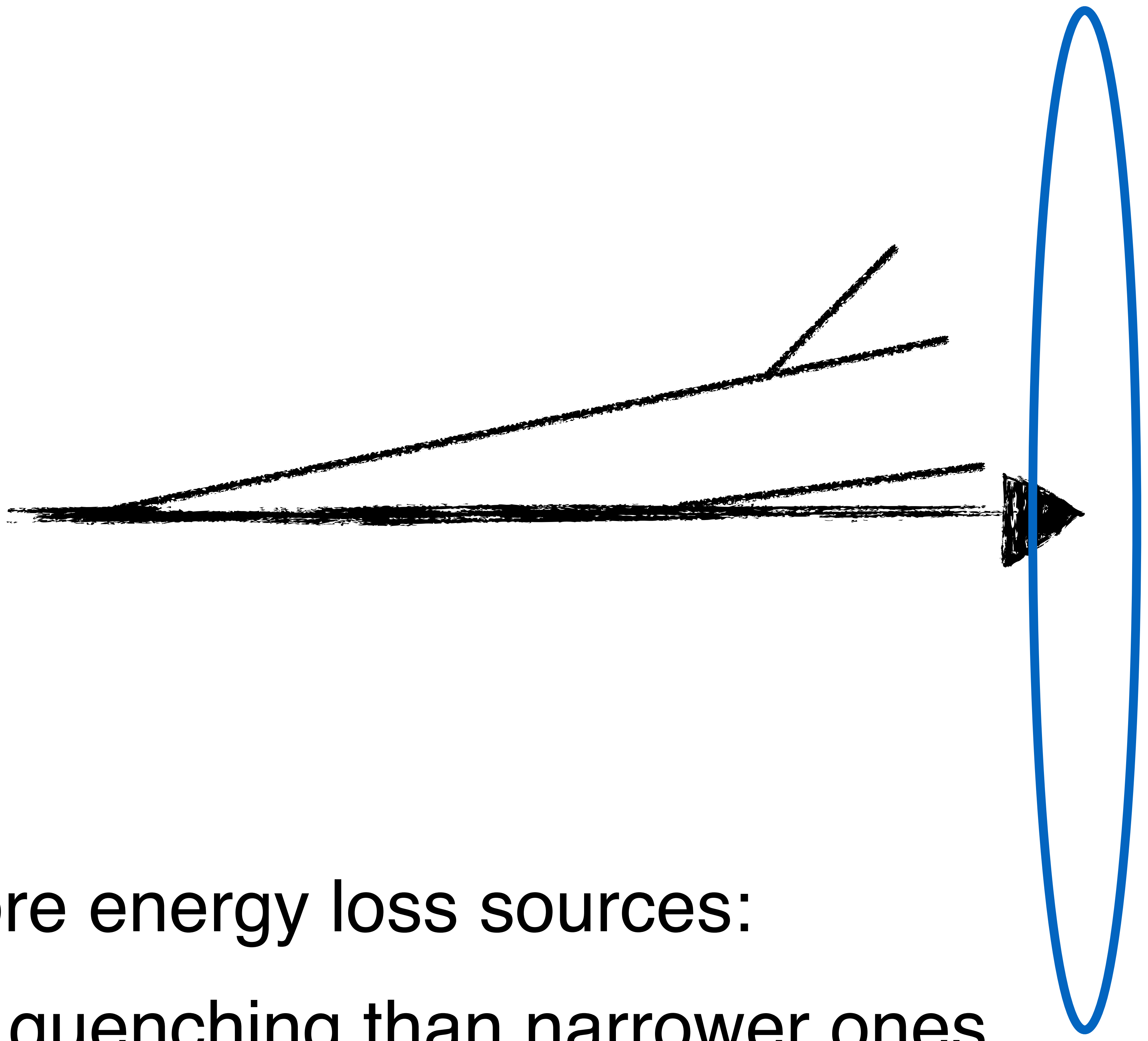

- Same energy.
- Same jet radius R.
- Different fragmentation pattern.

Wider jets have more energy loss sources:

→ more total quenching than narrower ones.

Assuming:

- most of the energy goes out of the cone.
- internal structure resolved by QGP.

Wide jet

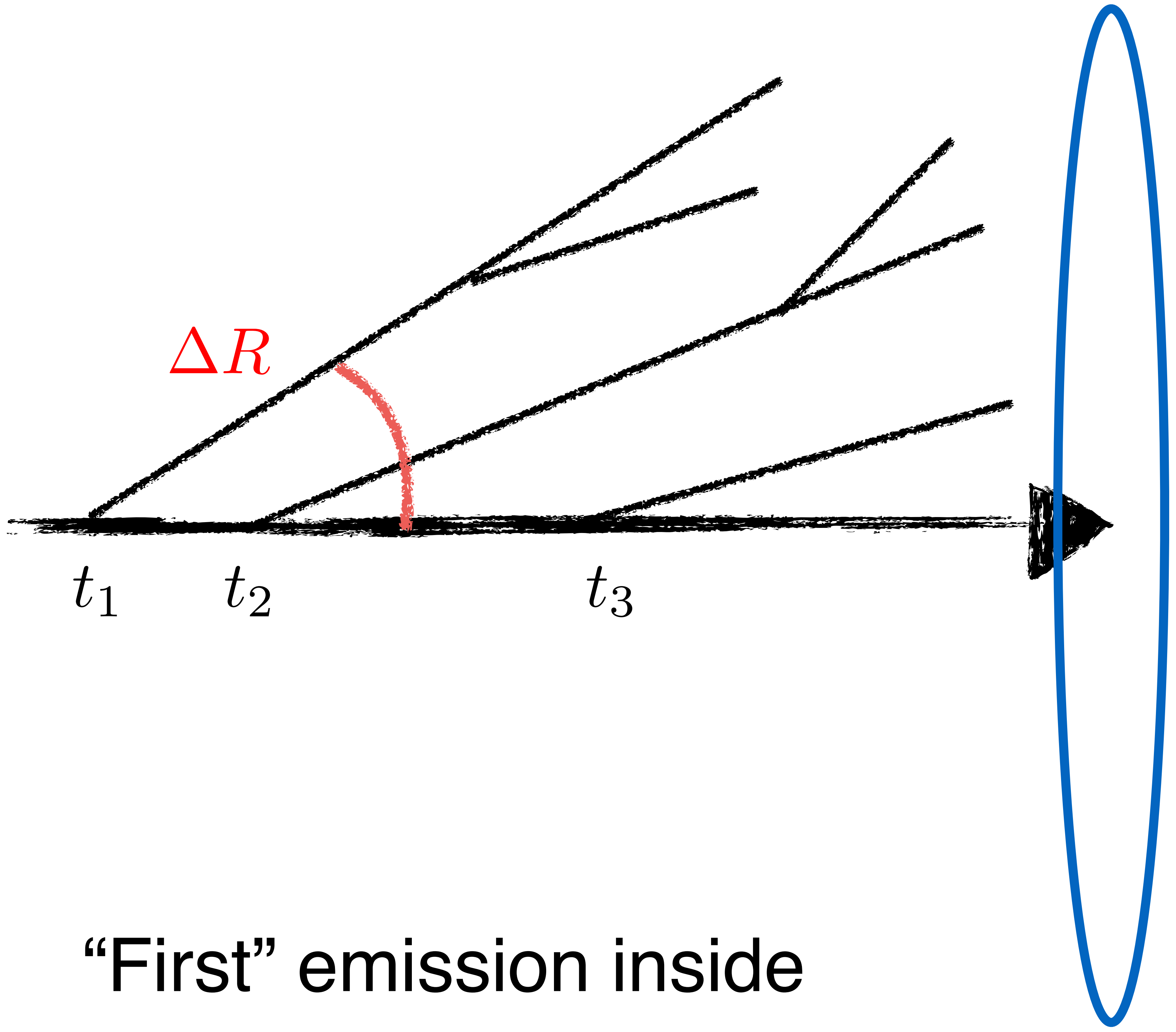

"First" emission inside the jet cone determines available phase space for further in-cone emissions.

Scale of emission *t* sampled from Sudakov distribution.

$$t_1 > t_1'$$

Groomed angle is proxy for jet activity.

Narrow jet

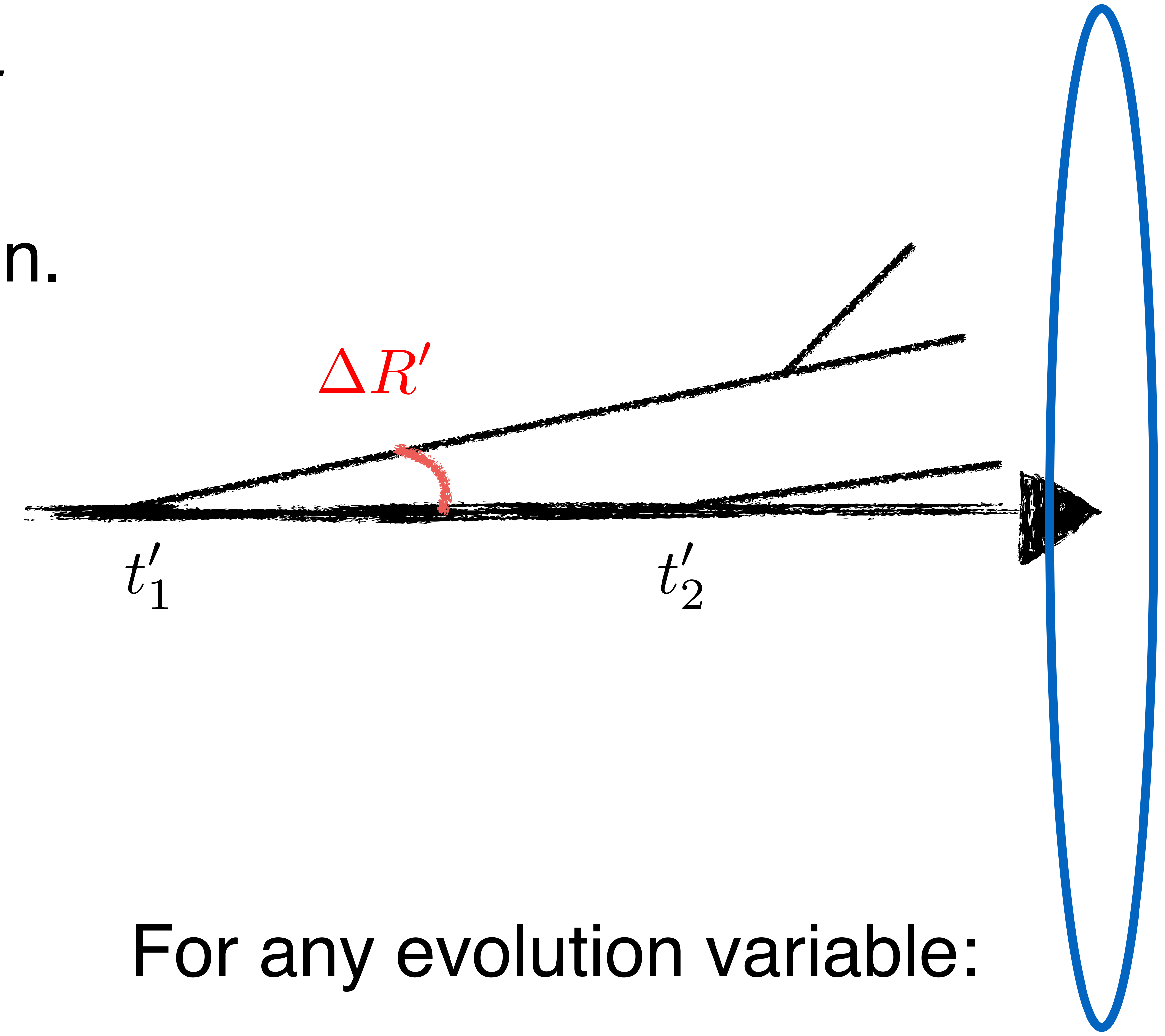

For any evolution variable:

$$t_1 \propto \Delta R$$
$$t_1' \propto \Delta R'$$

Correlation between n_{SD} and ΔR

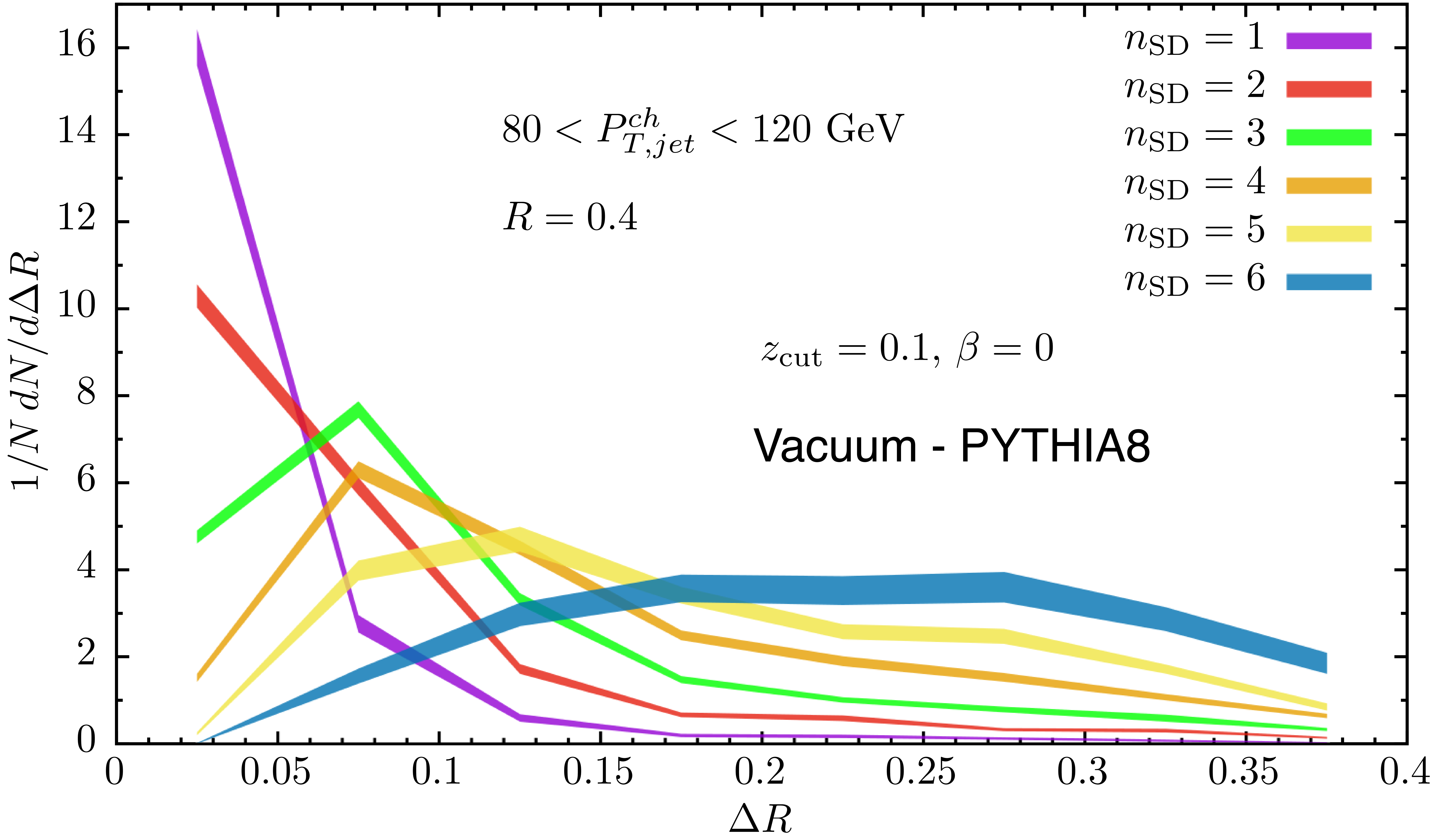

Casalderrey-Solana, Milhano, DP, Rajagopal, JHEP '20

Common feature among MC models

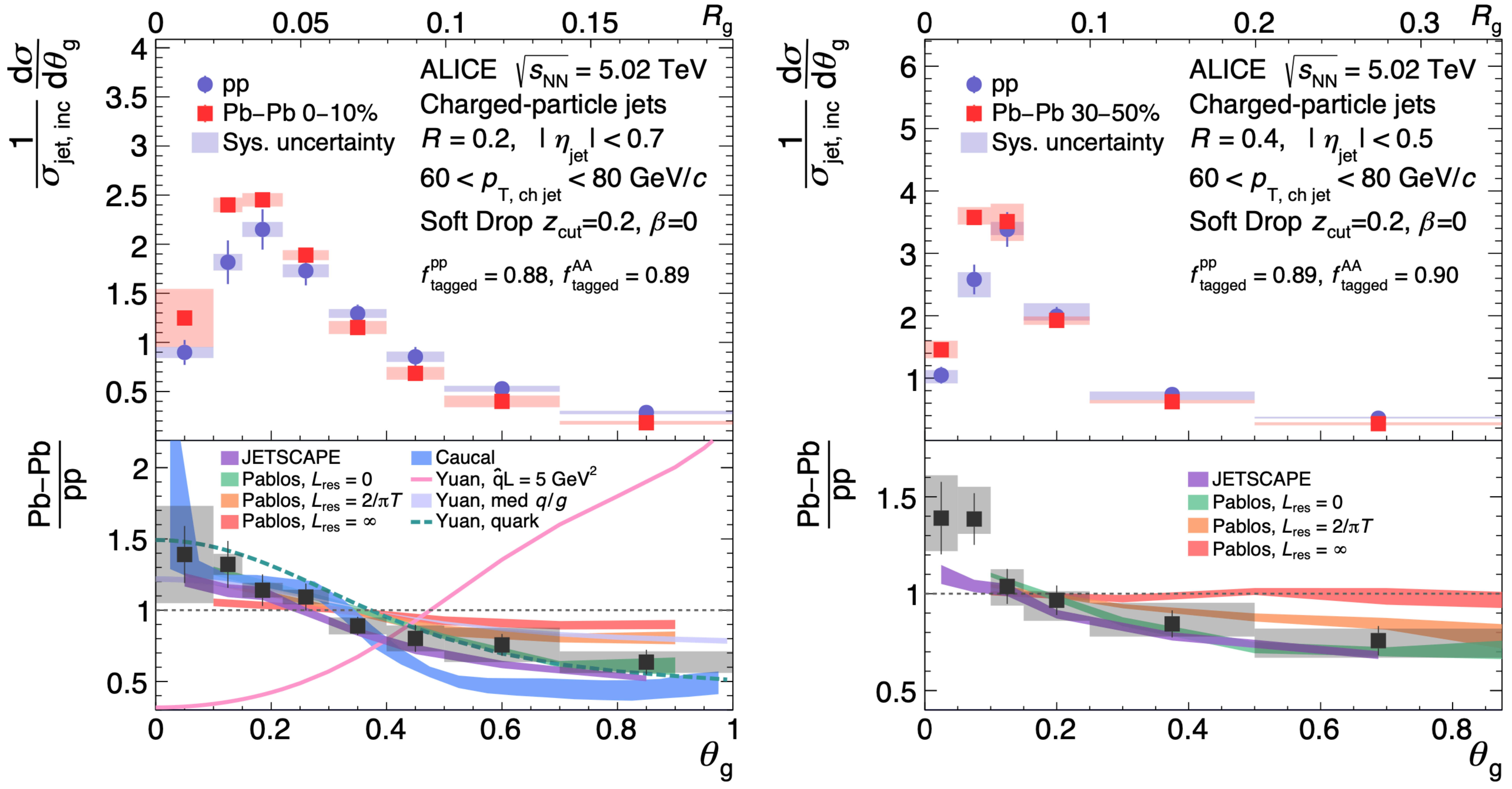

ALICE - PRL '22

ΔR narrowing observed in data, well reproduced by variety of models.

Most relevant common feature between MCs:

→ dominance of vacuum physics at early, high energy stages of the shower.

Modified q/g Fraction

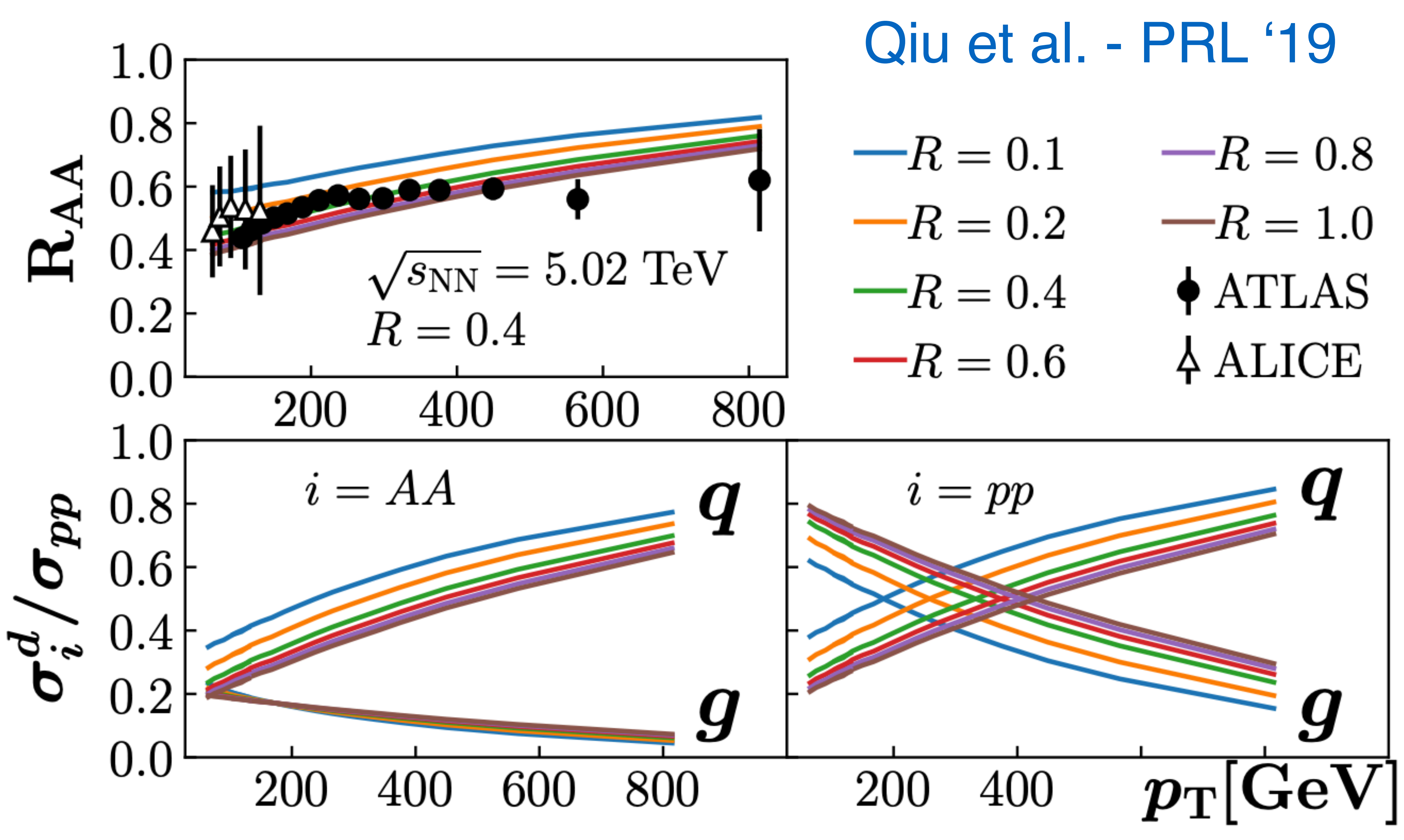

- Parameterization of modification of jet function (similar to nPDF).

$$\mu \frac{d}{d\mu} J_c(z, p_T R, \mu) = \sum_d P_{dc}(z) \otimes J_d(z, p_T R, \mu)$$

$$J_c^{\rm med}(z, p_T R, \mu_J) = W_c(z) \otimes J_c(z, p_T R, \mu_J)$$

$$W_c(z) = \epsilon_c \delta(1-z) + N_c\, z^{\alpha_c}(1-z)^{\beta_c}$$

→ Best fit seems to leave quark jets untouched.

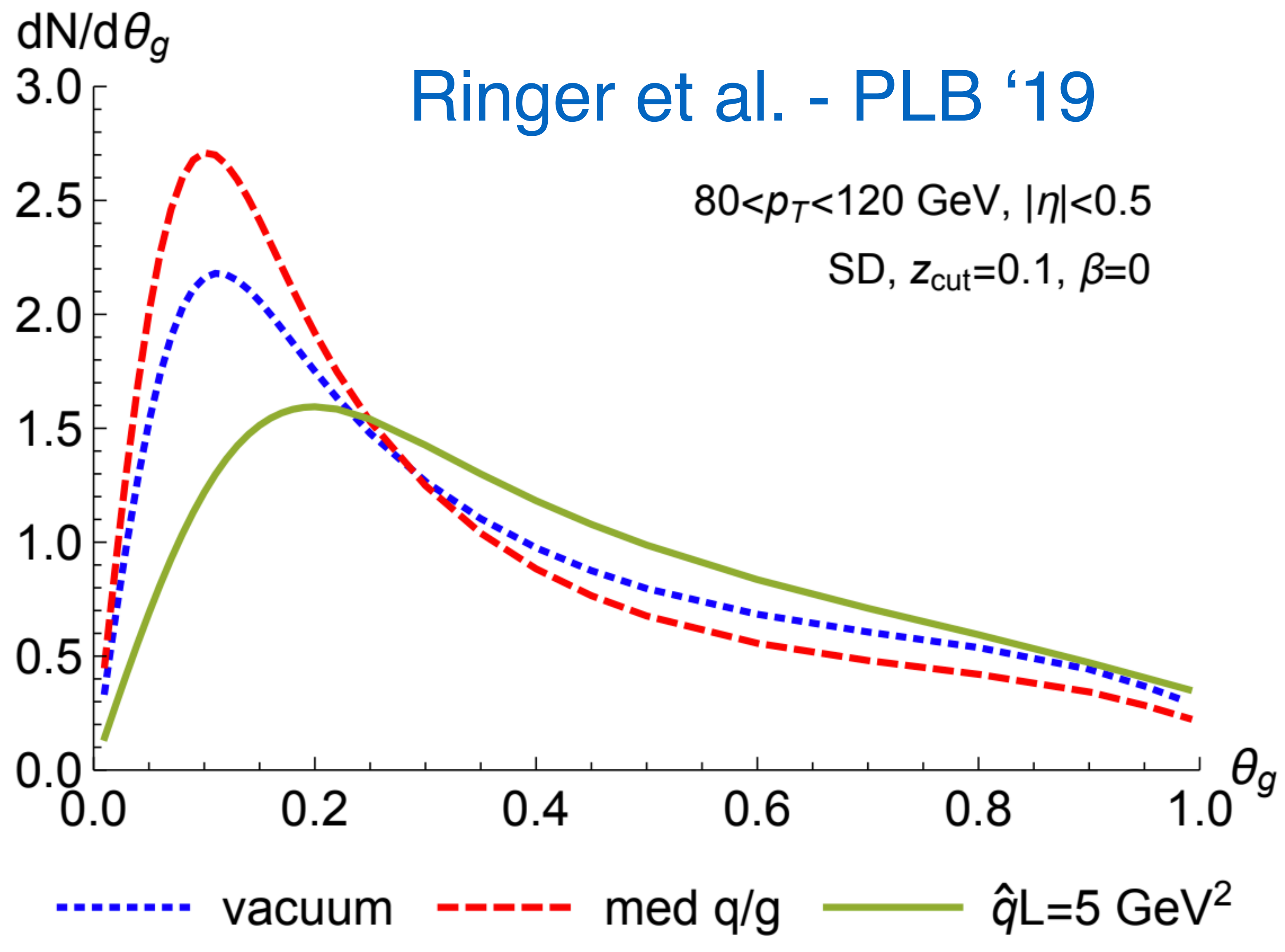

- Combination of quark and gluon contributions:

$$\frac{1}{\sigma_{\rm incl}} \frac{d\Sigma(\theta_g)}{dp_T\, d\eta} = f_q\, \Sigma_q(\theta_g) + f_g\, \Sigma_g(\theta_g)$$

- Broadening added as non-perturbative kick.

Substructure dependent jet suppression

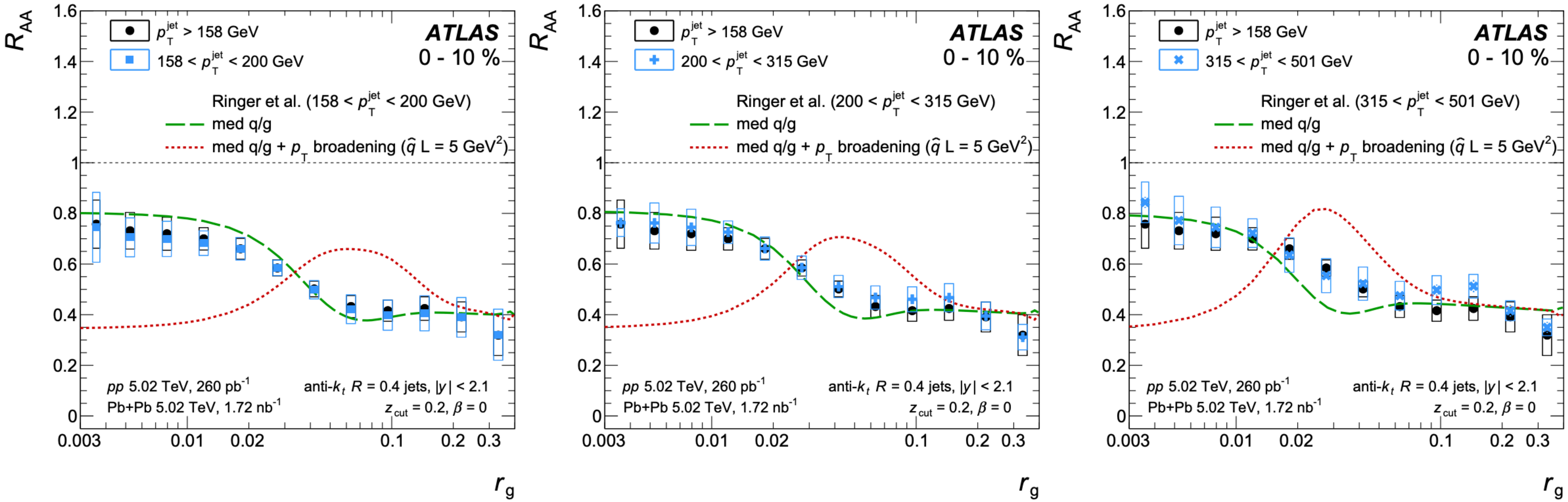

ATLAS - 2211.11470

Martin's talk on Tue

- Recent ATLAS results for R_{AA} vs r_g can also be explained by modified q/g fraction model.

Narrowing of Jet Substructure

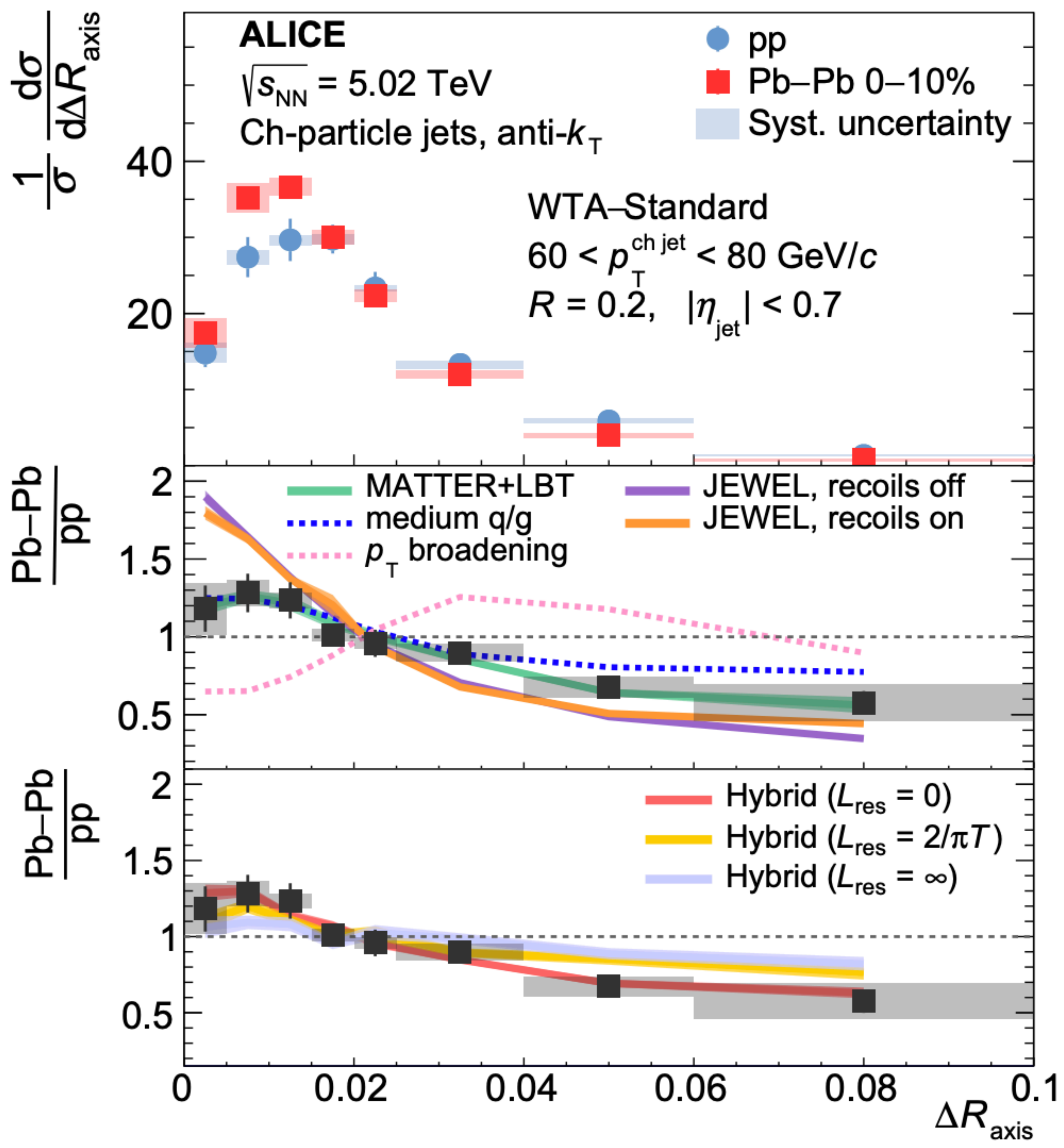

ALICE, 2303.13347

Rey's talk on Tue

How can we discriminate between:

- Quenching of wider jets, either quark or gluon (medium sensitive to jet substructure fluctuations).
- Modification of q/g fraction (medium sensitive to total charge only).

Simple proposal:

→ Use an enriched quark sample, so that over-quenching of gluons has very little effect.

Rapidity Evolution of Quark Fraction

DP & A. Soto-Ontoso - 2210.07901

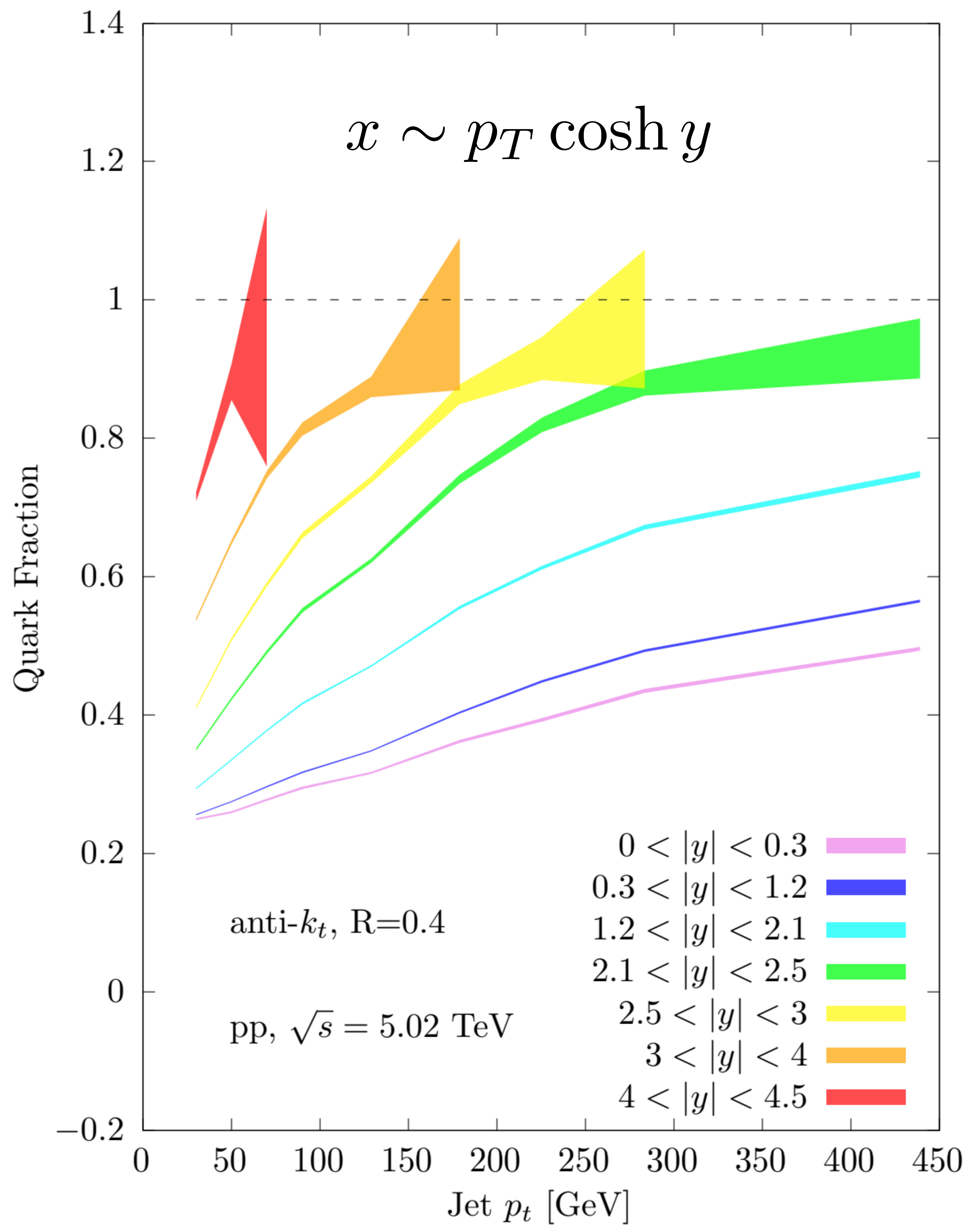

- Quark enriched samples can be obtained from e.g. inclusive b-tagged jets, semi-inclusive boson-jets.

- Here: exploit rapidity evolution of quark fraction to engineer quark enriched samples.

Extended rapidity coverages available in future detector upgrades.

ALICE3

Also ATLAS and CMS.

STAR

Forward Rapidity Upgrade
$2.5 < \eta < 4$

Leading-k_t at DLA in Vacuum

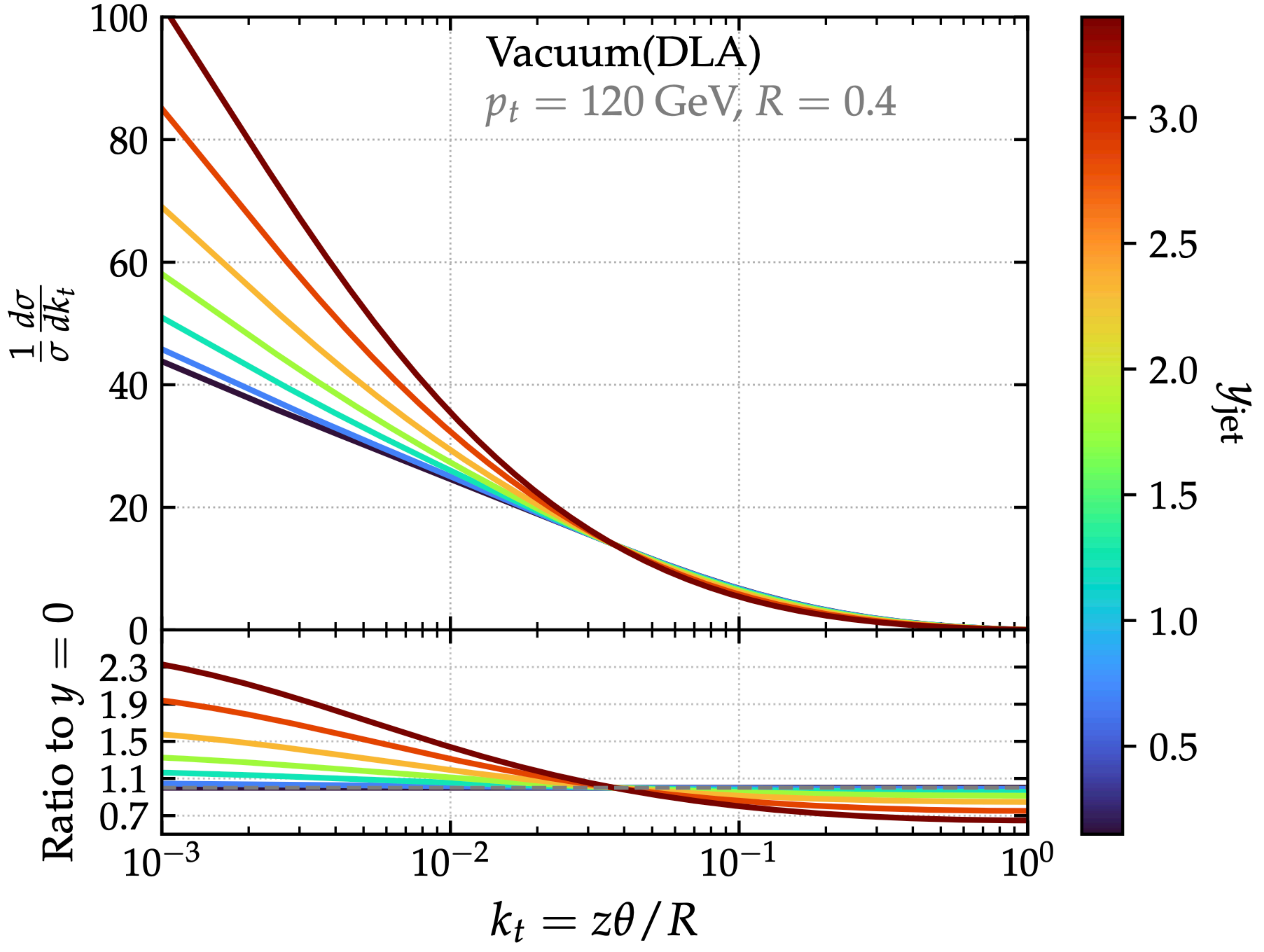

$$\frac{1}{\sigma}\frac{\mathrm{d}\sigma}{\mathrm{d}k_t}\bigg|_{p_t,y} = \sum_{i\in\{q,g\}} f_i \int_0^1 \mathrm{d}z \int_0^R \mathrm{d}\theta P^{\mathrm{vac}}(z,\theta)\delta(k_t - z\theta)$$

$$\times\, e^{-\int \mathrm{d}z' \int \mathrm{d}\theta' P^{\mathrm{vac}}(z',\theta')\Theta(z'\theta' - k_t)}$$

$$\overset{\mathrm{DLA}}{=} \sum_{i\in\{q,g\}} f_i \frac{2\bar{\alpha}}{k_t} \ln\frac{R}{k_t} e^{-\bar{\alpha}\ln^2\frac{R}{k_t}}$$

$$\bar{\alpha} \equiv \alpha_s(p_t R)C_i/\pi$$

Vacuum q/g fractions; taken from PYTHIA8.

Probability of measuring splitting with k_t.

Probability there is no other splitting with larger value of k_t (Sudakov factor).

Total distribution becomes narrower at forward rapidities as q-fraction increases.

DP & A. Soto-Ontoso - 2210.07901

Leading-k_T Distribution in pp

$$k_t \equiv z p_t^{\text{parent}} \sin\theta$$

DP & A. Soto-Ontoso - 2210.07901

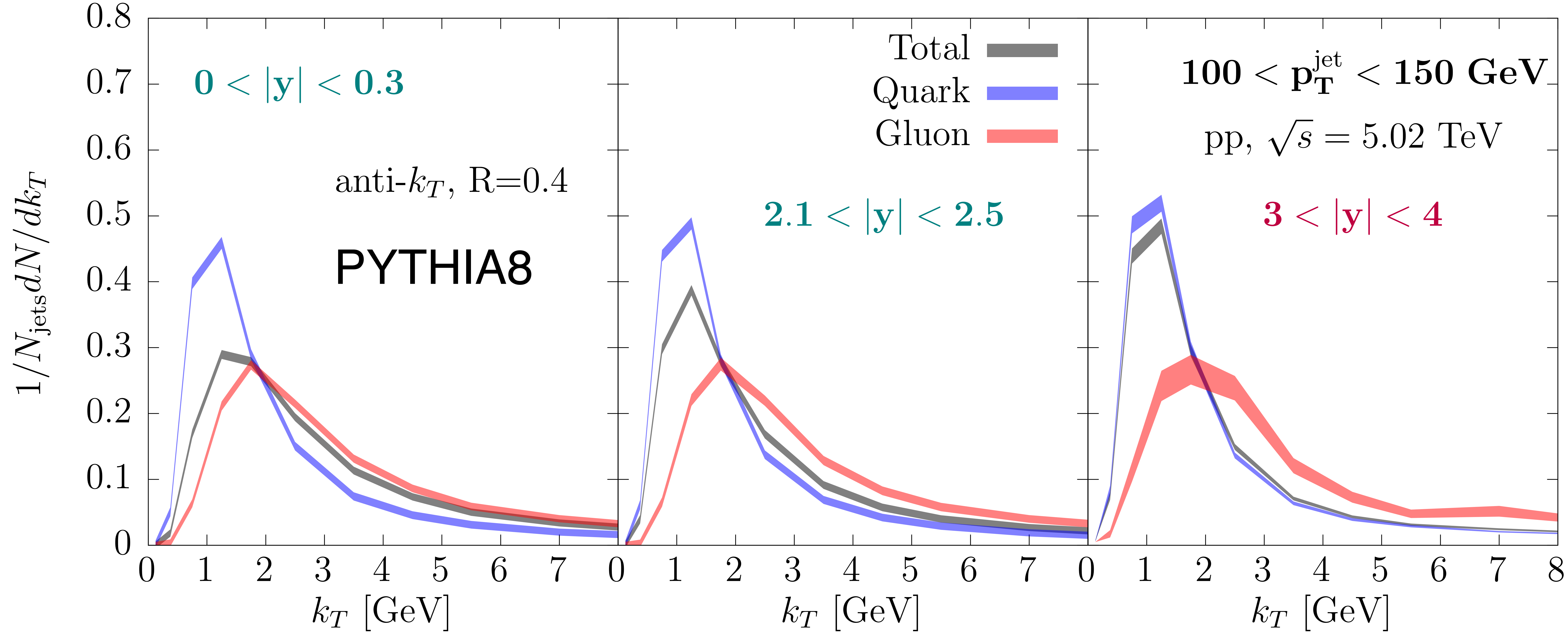

- Compute leading-k_t in a C/A reclustered tree.

→ Distribution for quark jets narrower than for gluon jets.

→ Moving to forward rapidities, sample dominated by quark jets.

In-Medium Jet Propagation

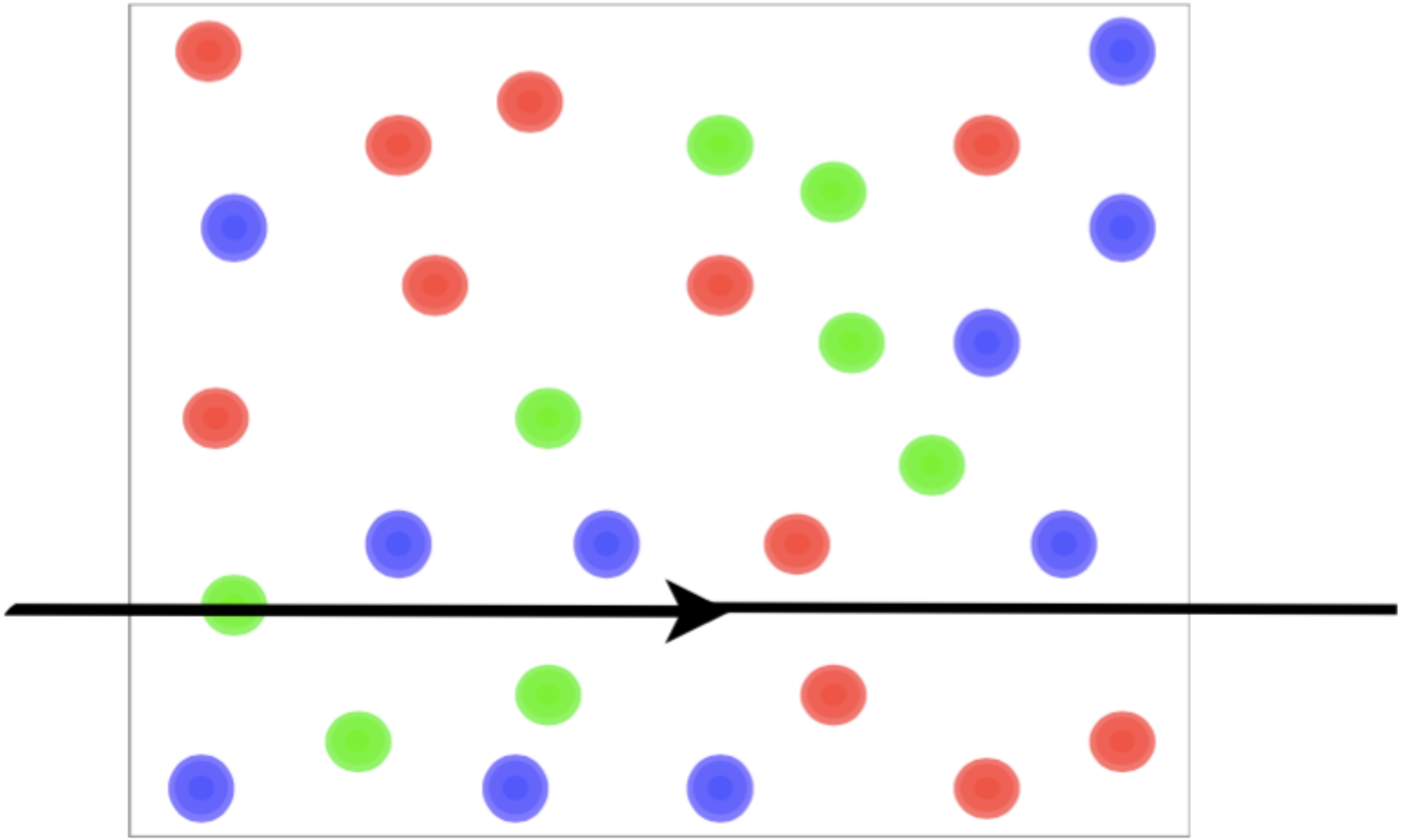

In-Medium Jet Propagation

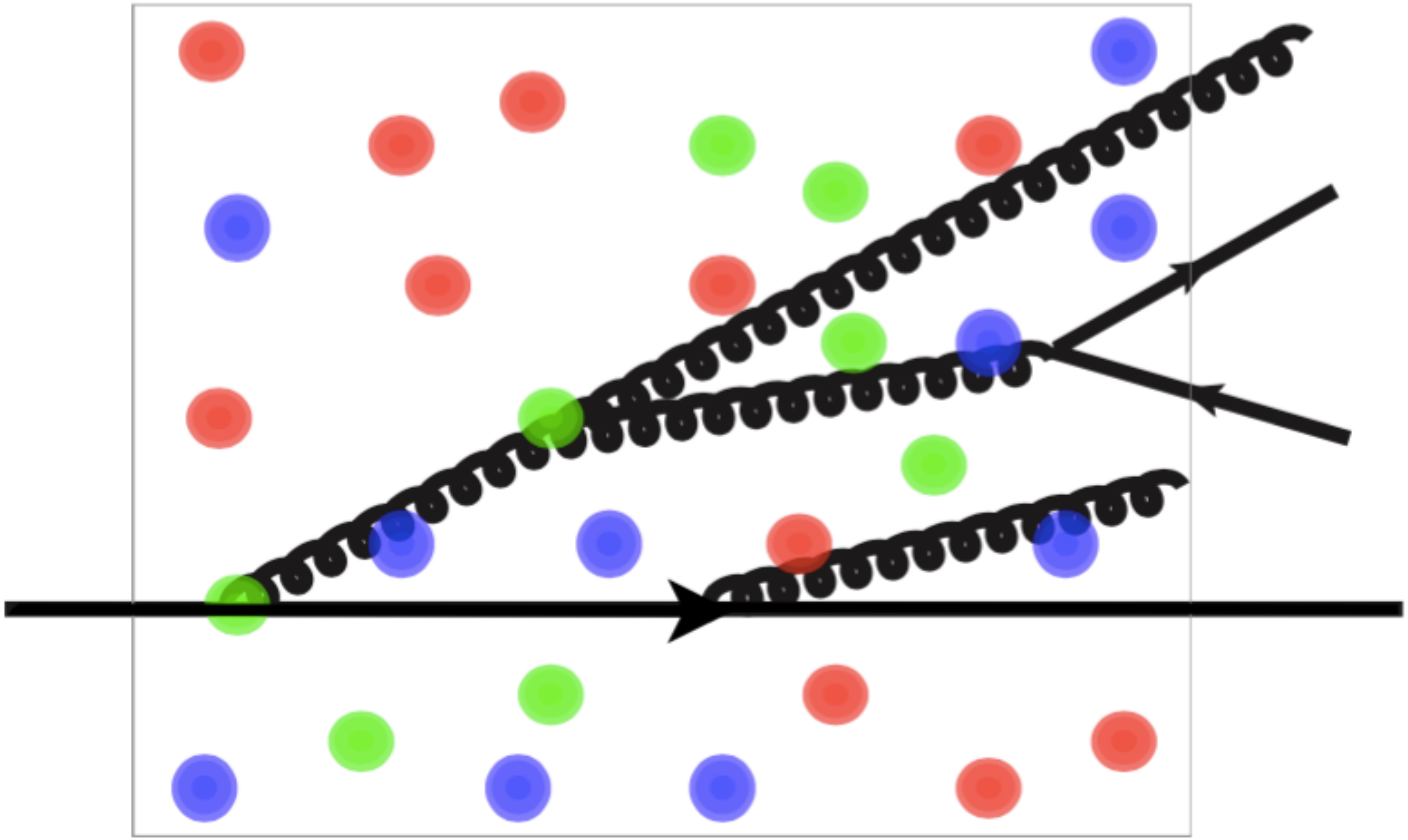

Coherence Effects

QGP resolution length:

minimal distance between two coloured charges such that they engage with the plasma independently. → The medium perceives a parton shower as a collection of effective probes.

At weak coupling:
connection between resolution length and energy loss.

At strong coupling:
no such connection (yet).

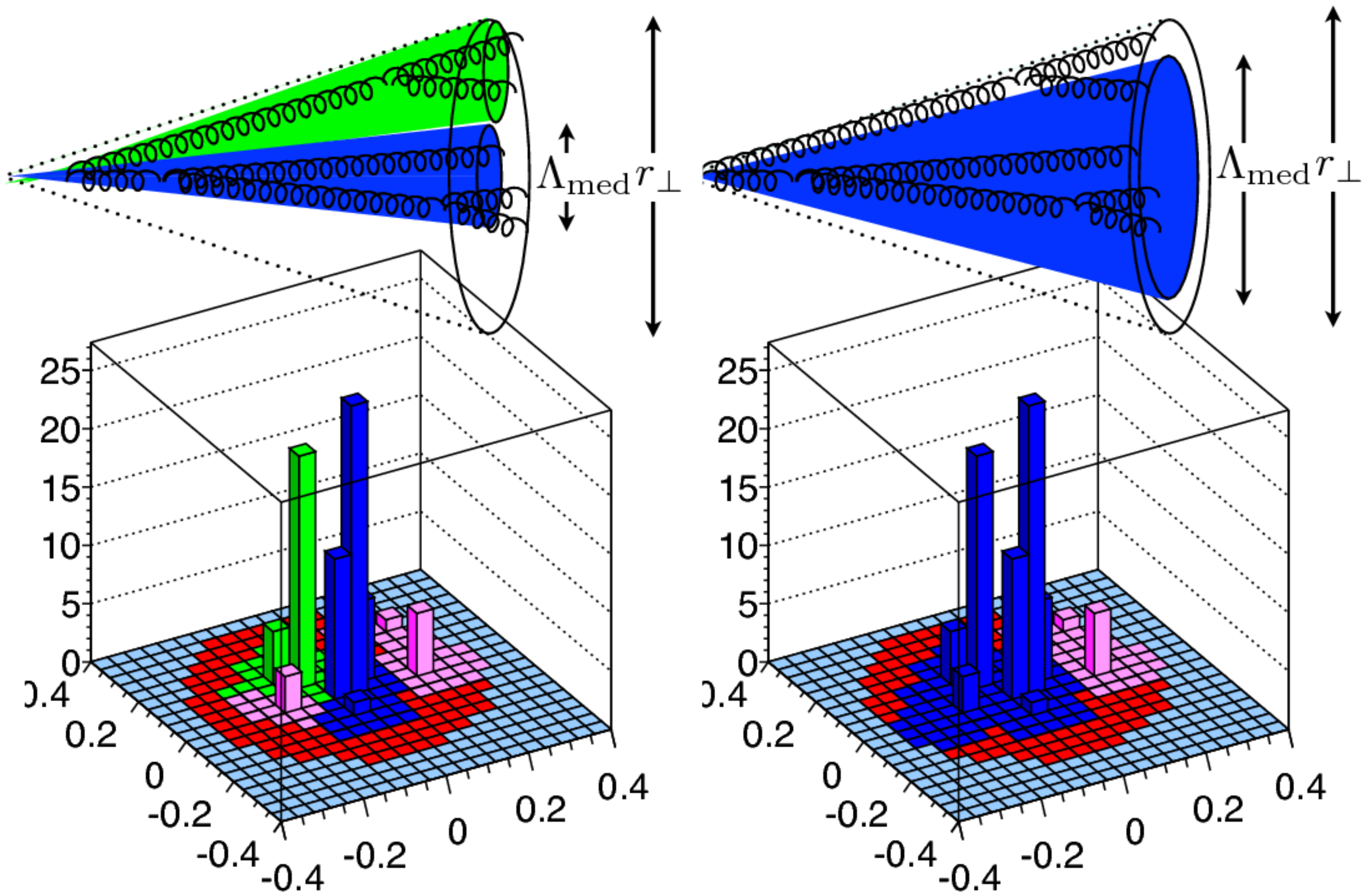

Casalderrey et al. - PLB ‘13

At weak coupling:
Antenna can lose coherence due to color rotations via multiple soft scatterings with the medium.

Decoherence time $t_{\rm coh}(\theta_{q\bar{q}}) \equiv \left(\frac{4}{\hat{q}\theta_{q\bar{q}}^2}\right)^{1/3}$

For maximum possible length L, minimal angle

$$\theta_c \equiv 2/\sqrt{\hat{q}L^3}$$

Quenched Phase Space of a Jet

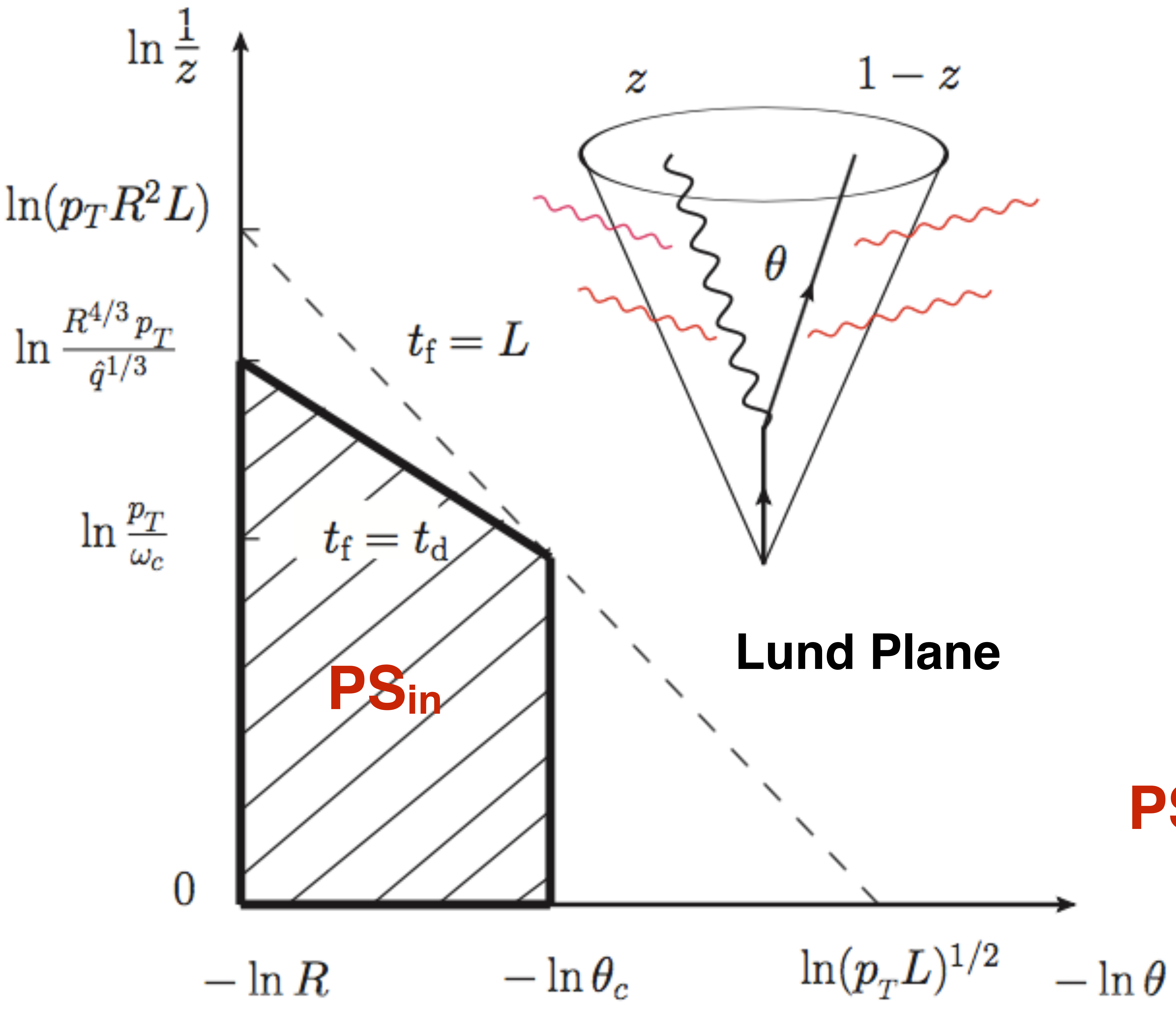

- Only those jet modes that:
  - are formed inside the medium, and,

$$t_f < L$$

  - are resolved by the medium,

$$t_f < t_d$$

contribute to double-logarithmic enhancement of quenched phase space:

$$\mathbf{PS_{in}} = \bar{\alpha} \int_{t_f < t_d < L} \frac{d\theta}{\theta} \int \frac{dz}{z} \equiv \bar{\alpha} \ln \frac{R}{\theta_c} \left(\ln \frac{p_T}{\omega_c} + \frac{2}{3} \ln \frac{R}{\theta_c} \right)$$

Mehtar-Tani, Tywoniuk - PRD '18

see also Caucal, Iancu, Mueller, Soyez - PRL '18

Analytic q/g frac. model at DLA

DP & A. Soto-Ontoso - 2210.07901

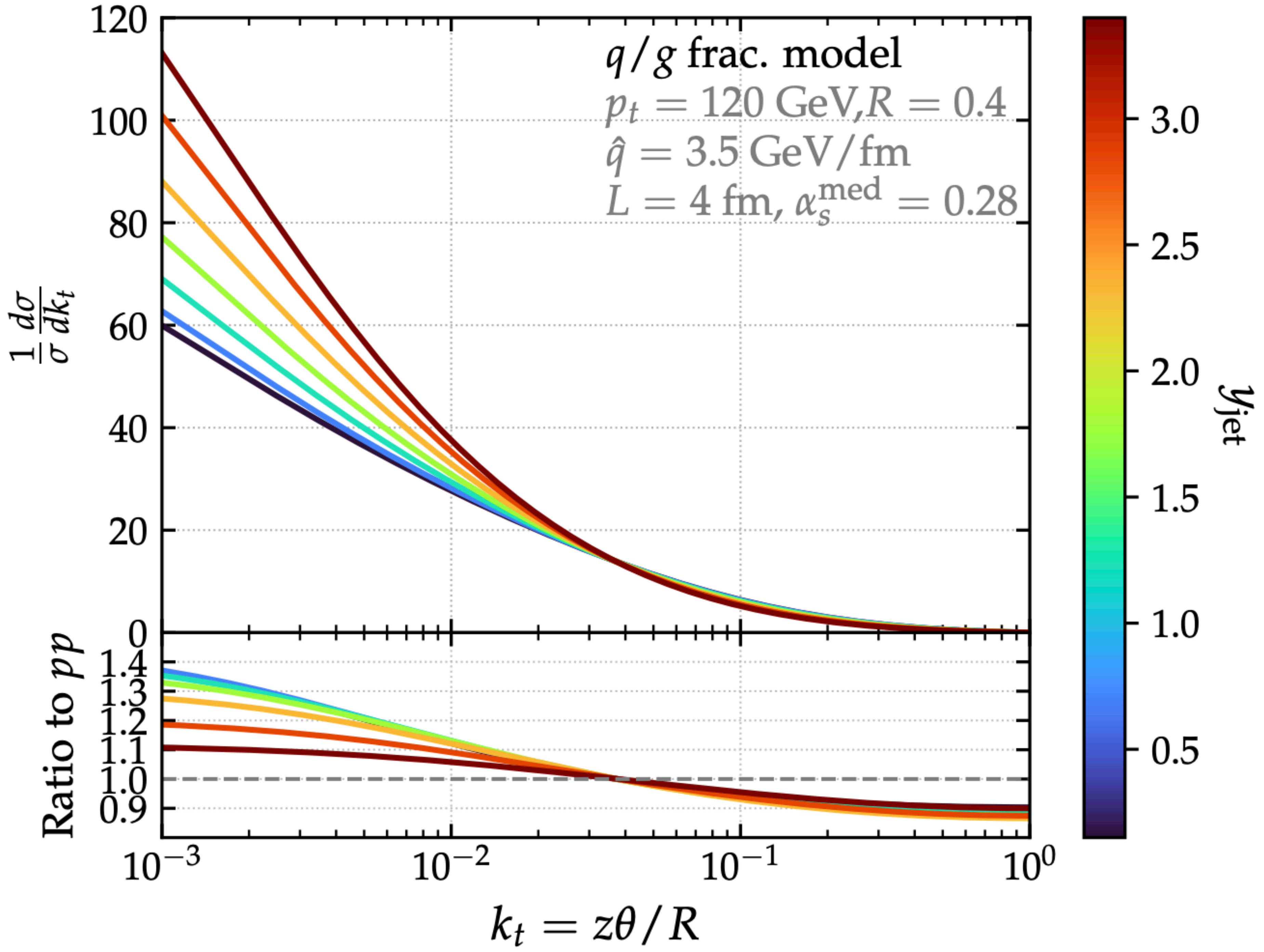

Less narrowing with increasing rapidity.

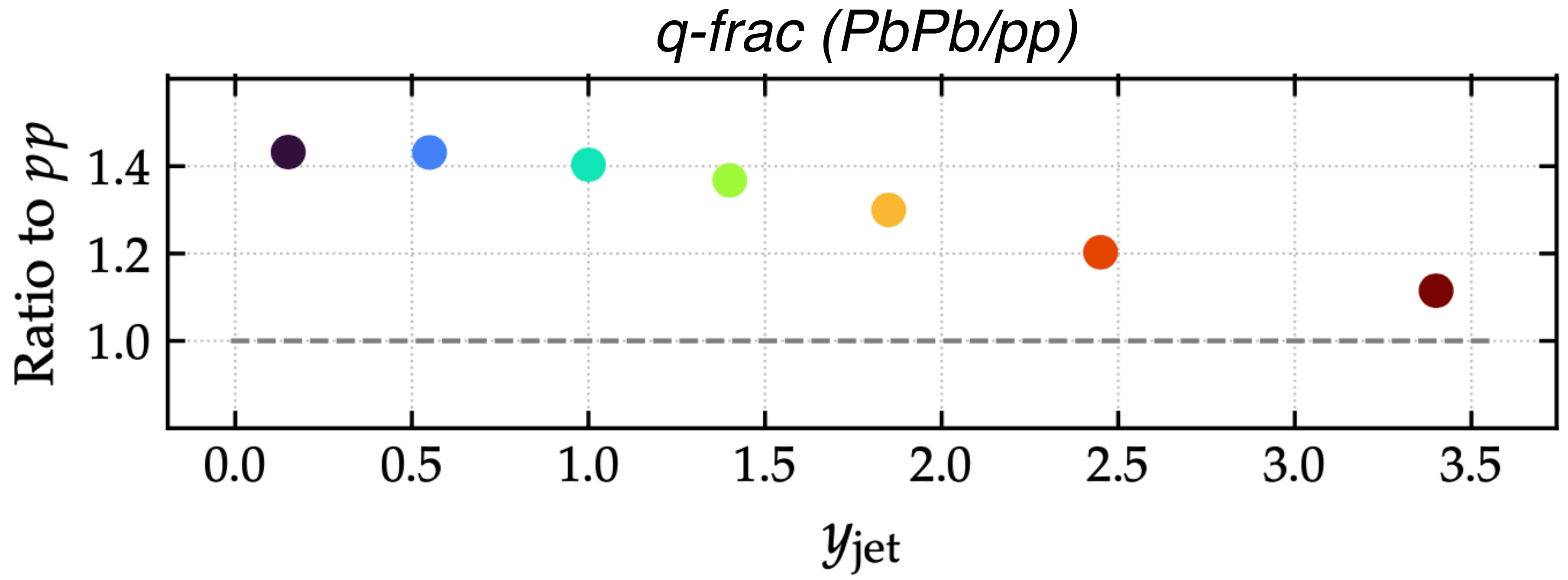

nPDF-modified q/g fractions (small effect)

$$\frac{1}{\sigma}\frac{d\sigma}{dk_t}\bigg|_{p_t,y} = \frac{1}{\mathcal{N}}\sum_{i\in\{q,g\}} f_i^{\rm n}\int_0^1 dz\int_0^R d\theta P_i^{\rm med}(z,\theta) \times e^{-\int dz'\int d\theta' P^{\rm med}(z',\theta')\Theta(z'\theta'-k_t)}\delta(k_t - z\theta) \times \int_0^\infty d\varepsilon\mathcal{E}_i(\varepsilon|z,\theta)e^{-\frac{n\varepsilon}{p_t}}$$

Energy loss BDMPS-Z

q/g frac model:

Triggered splitting assumed vacuum-like only.

$$\rightarrow P^{\rm med} \to \bar{\alpha}/(z\theta)$$

Quenching of leading charge only.

$$\rightarrow \mathcal{Q}_i(p_t,R) \equiv \int_0^\infty d\varepsilon\mathcal{E}_i(\varepsilon|z,\theta)e^{-\frac{n\varepsilon}{p_t}}$$

(Note: effect at mid-rapidity not as big as Ringer et al., different medium q/g fraction).

Analytic decoherence model at DLA

DP & A. Soto-Ontoso - 2210.07901

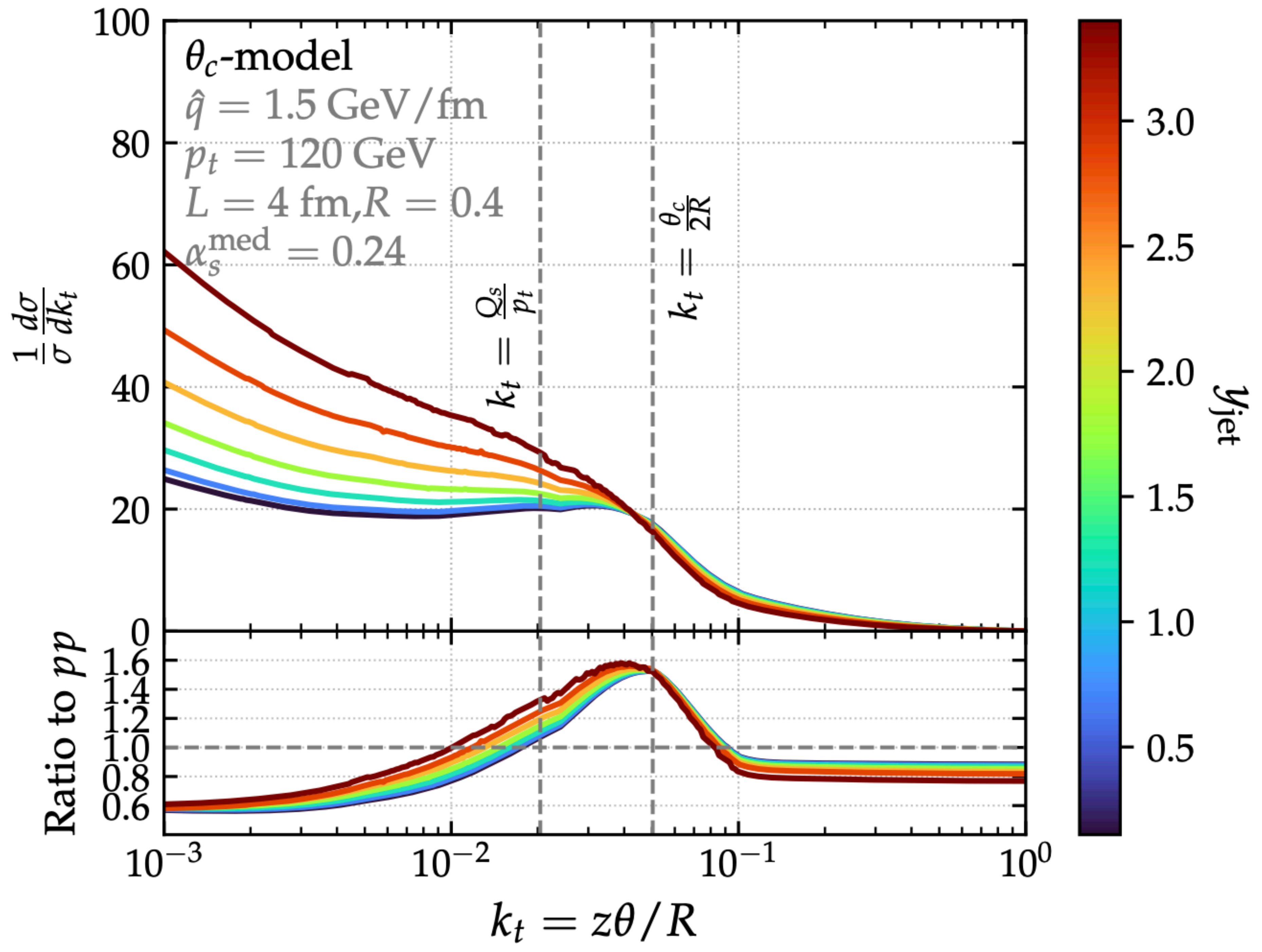

Narrowing persists also at forward rapidities.

nPDF-modified q/g fractions (small effect)

$$\frac{1}{\sigma}\frac{d\sigma}{dk_t}\bigg|_{p_t,y} = \frac{1}{\mathcal{N}}\sum_{i\in\{q,g\}} f_i^{\rm n}\int_0^1 dz\int_0^R d\theta P_i^{\rm med}(z,\theta)$$
$$\times\, e^{-\int dz'\int d\theta' P^{\rm med}(z',\theta')\Theta(z'\theta'-k_t)}\delta(k_t - z\theta)$$

Energy loss BDMPS-Z

$$\times \int_0^\infty d\varepsilon\, \mathcal{E}_i(\varepsilon|z,\theta) e^{-\frac{n\varepsilon}{p_t}}$$

θ_c model:

Triggered splitting can be medium-induced.

$$\rightarrow\ P^{\rm med}(z,\theta) = P^{\rm vac}(z,\theta)\Theta_{\notin \rm veto}(z,\theta) + P^{\rm mie}(z,\theta)$$

Quenching of leading and tagged prongs if resolved (i.e. with $\theta > \theta_c$).

$$\rightarrow\ \int_0^\infty d\varepsilon\, \mathcal{E}_i(\varepsilon|z,\theta) e^{-\frac{n\varepsilon}{p_t}} = (1-\Theta_{\rm res})\mathcal{Q}_i(p_t,R) + \Theta_{\rm res}\mathcal{Q}_g(p_t,R)\mathcal{Q}_i(p_t,R)$$

$$\Theta_{\rm res}(z,\theta) = \Theta(\theta-\theta_c)\Theta(k_t - k_{t,\rm med})$$

Analytic Estimates at DLA - Summary

DP & A. Soto-Ontoso - 2210.07901

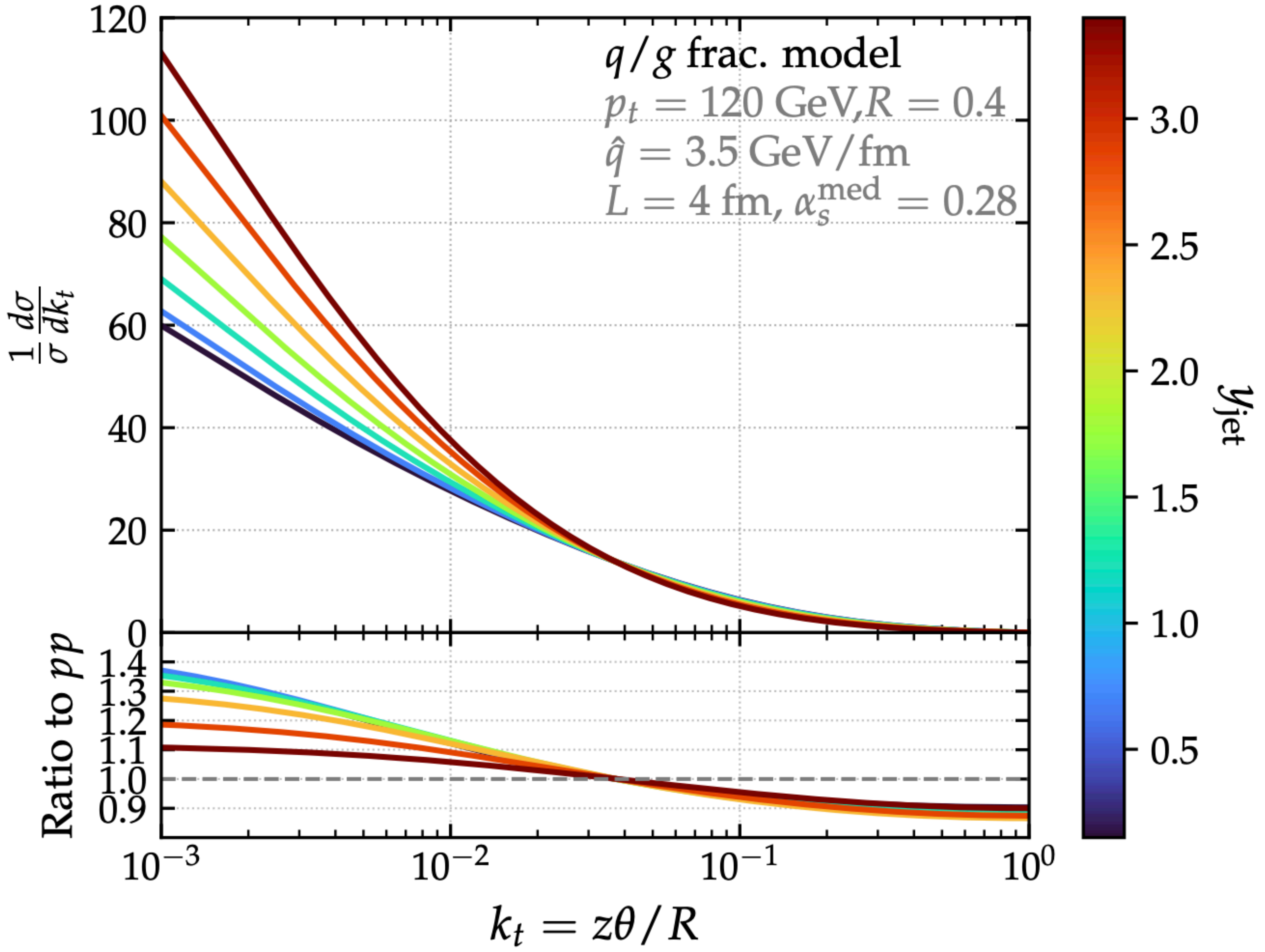

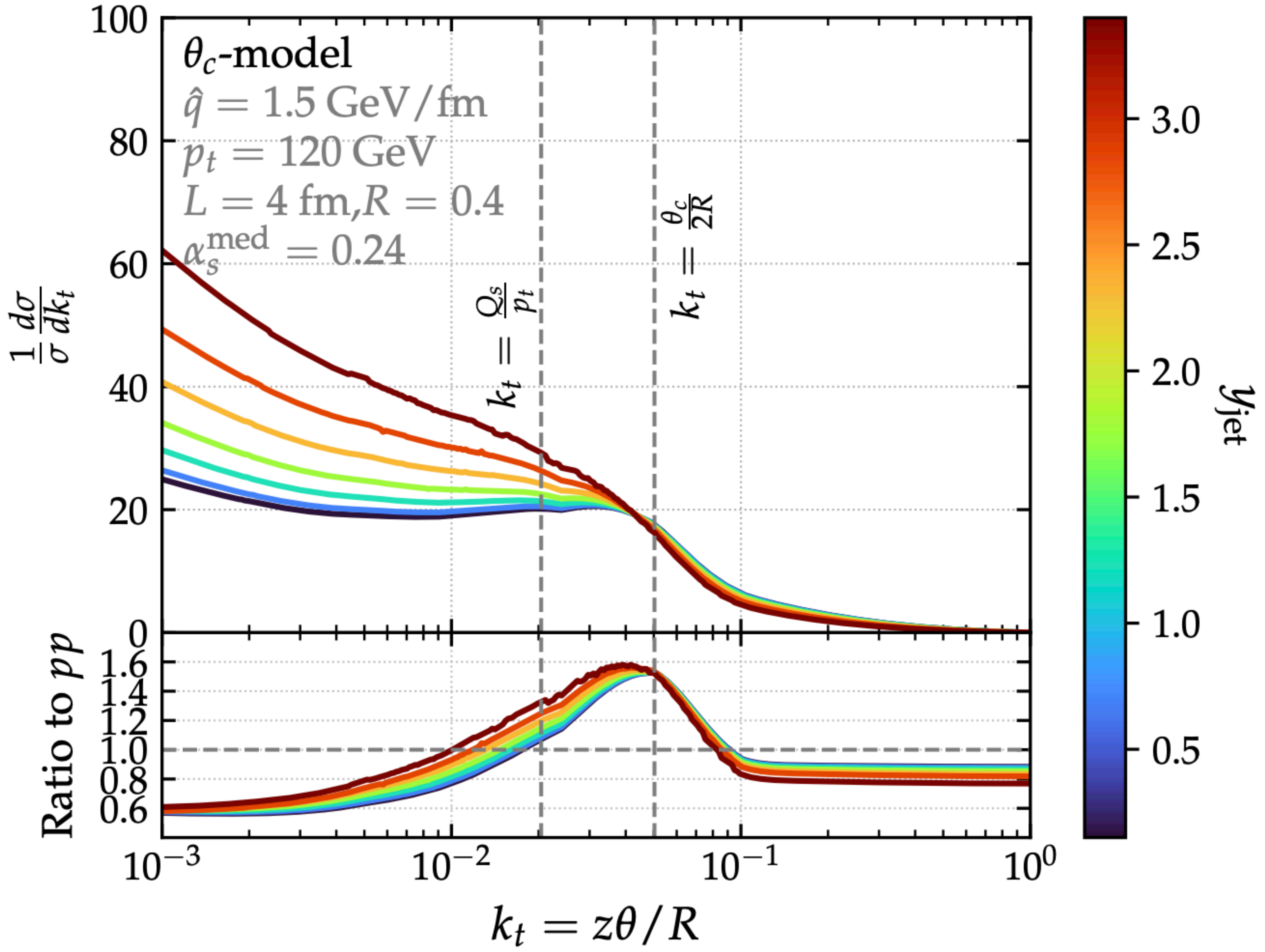

q/g frac model:

→ Quenching of leading charge only.

Less narrowing with increasing rapidity.

θ_c model:

→ Quenching of leading and tagged prongs if resolved (i.e. with $\theta > \theta_c$).

Narrowing persists also at forward rapidities.

Hybrid Strong/Weak Coupling Model

$$\frac{1}{E_{\rm in}}\frac{dE}{dx} = -\frac{4}{\pi}\frac{x^2}{x_{\rm stop}^2}\frac{1}{\sqrt{x_{\rm stop}^2 - x^2}}$$

$$x_{\rm stop} = \frac{1}{2\kappa_{\rm sc}}\frac{E_{\rm in}^{1/3}}{T^{4/3}}$$

$\mathcal{O}(1)$ free parameter

$$E\frac{d\Delta N}{d^3p} = \frac{1}{32\pi}\frac{m_T}{T^5}\cosh(y-y_j)\exp\left[-\frac{m_T}{T}\cosh(y-y_j)\right]$$
$$\left\{p_T\Delta P_T\cos(\phi-\phi_j) + \frac{1}{3}m_T\,\Delta M_T\,\cosh(y-y_j)\right\}$$

Strongly coupled
energy loss
(hydrodynamization rate)

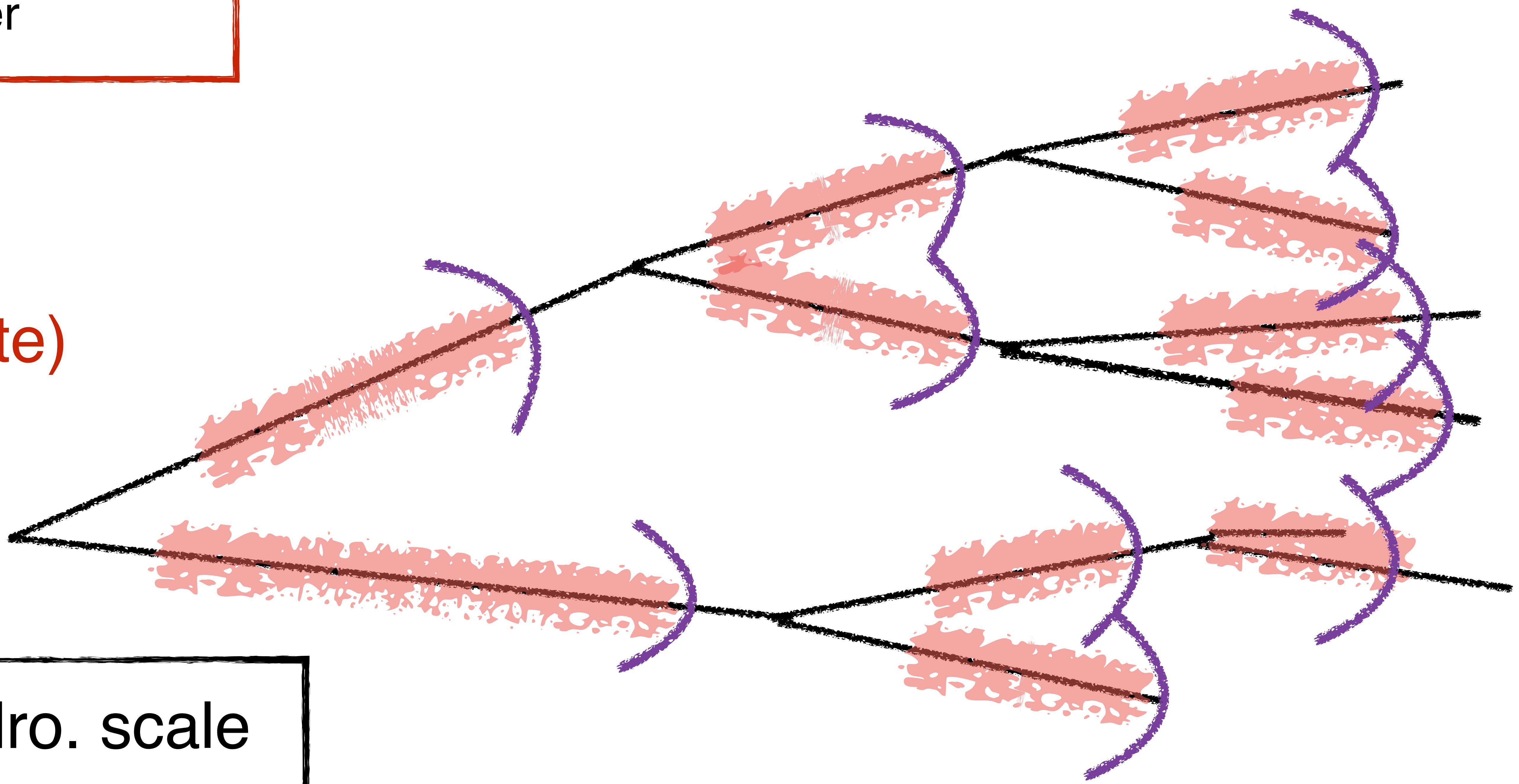

Hadrons from the hydro. wake (medium response)

Improved flow-dependent wake in the works.

See Jorge's talk on Tue

PYTHIA8 down to hadro. scale
(formation time argument
for spacetime picture)

Casalderrey-Solana, Gulhan, Milhano, DP, Rajagopal JHEP '15,'16,'17

Rapidity Dependence of R_{AA}

w/ boost invariant medium (good up to y~3)

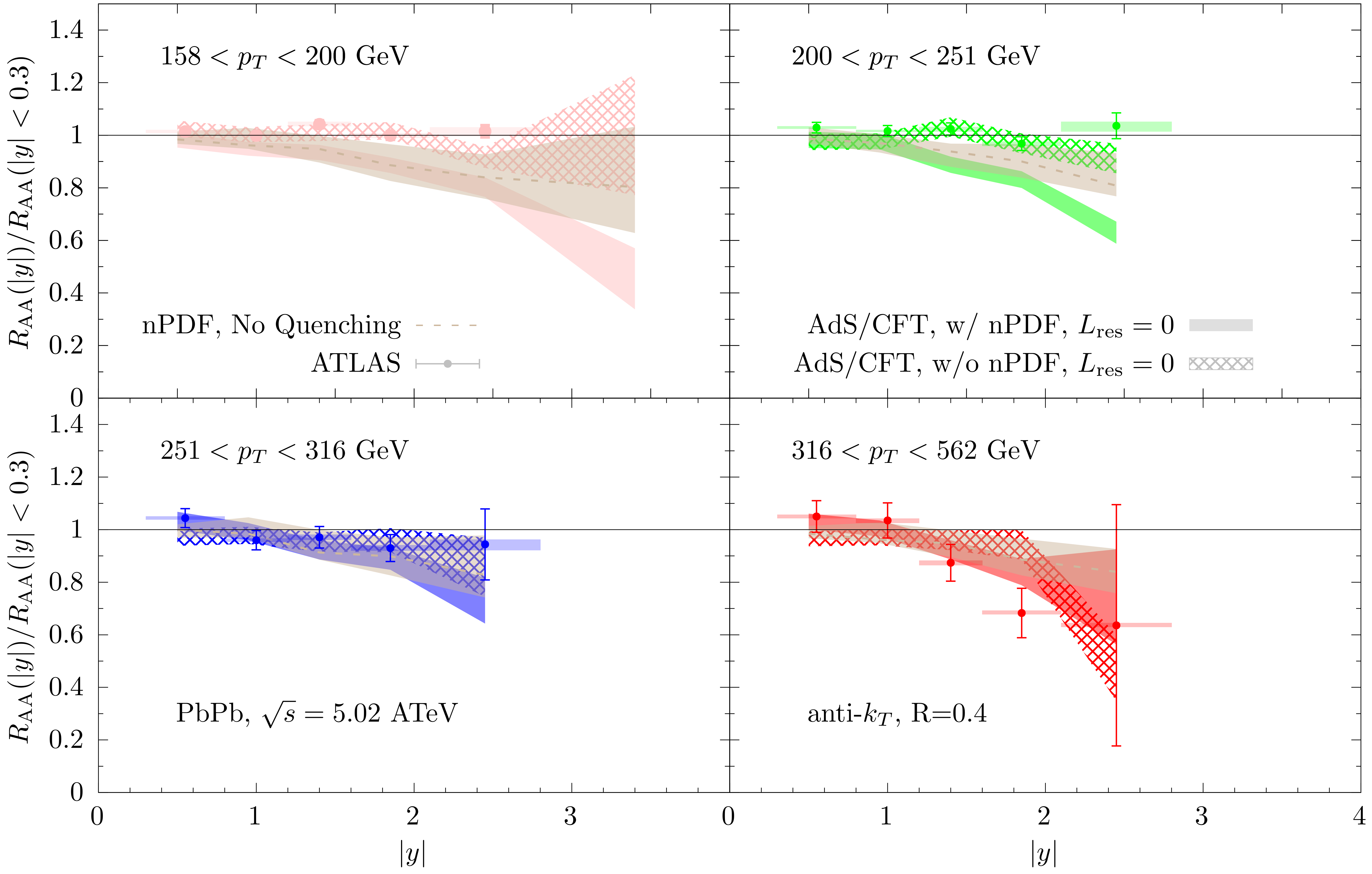

DP & A. Soto-Ontoso - 2210.07901

- Without nPDF, flatness of R_{AA} result of competing effects:
  Steepness of spectrum,
  change in q-fraction.
- Initial state effects affect R_{AA} vs rapidity.
  (Also observed in Adhya et al. - EPJC '22.)
- Need to check with updated sets EPPS21 and nNNPDF3.0.
  Differences among nPDF?
  Could we constrain nPDF?

Rapidity Depence of R_{AA}

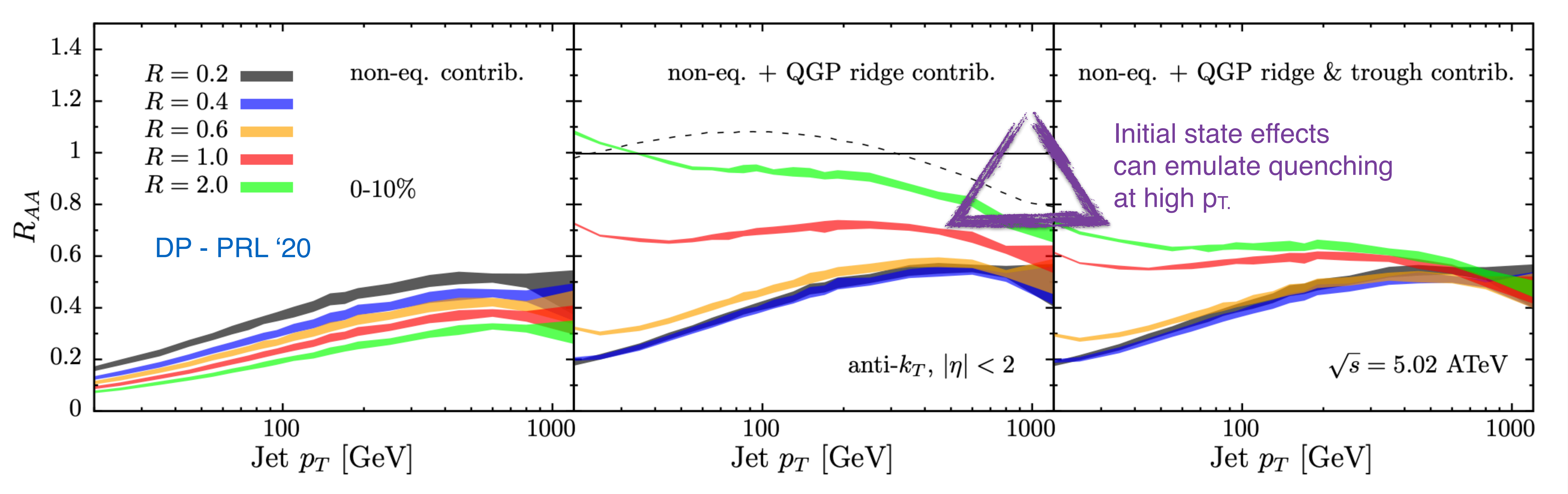

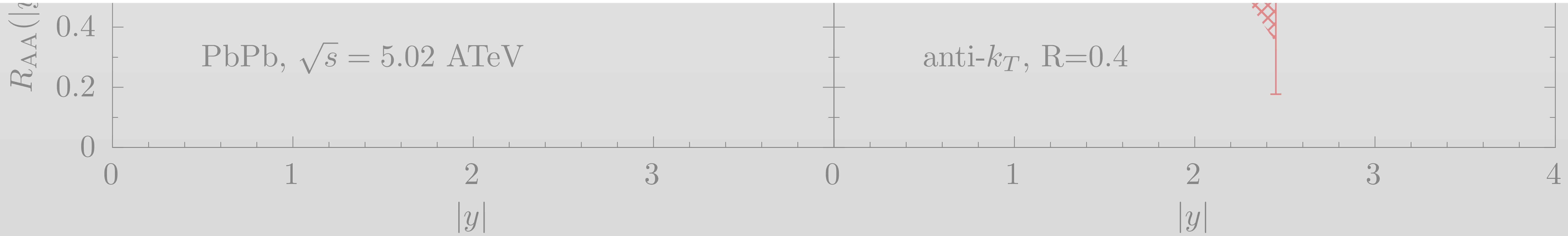

- Need to use updated sets EPPS21 and nNNPDF3.0.

  Differences?
  Could we constrain?

DP & A. Soto-Ontoso - 2210.07901

q-fraction in the Hybrid Model

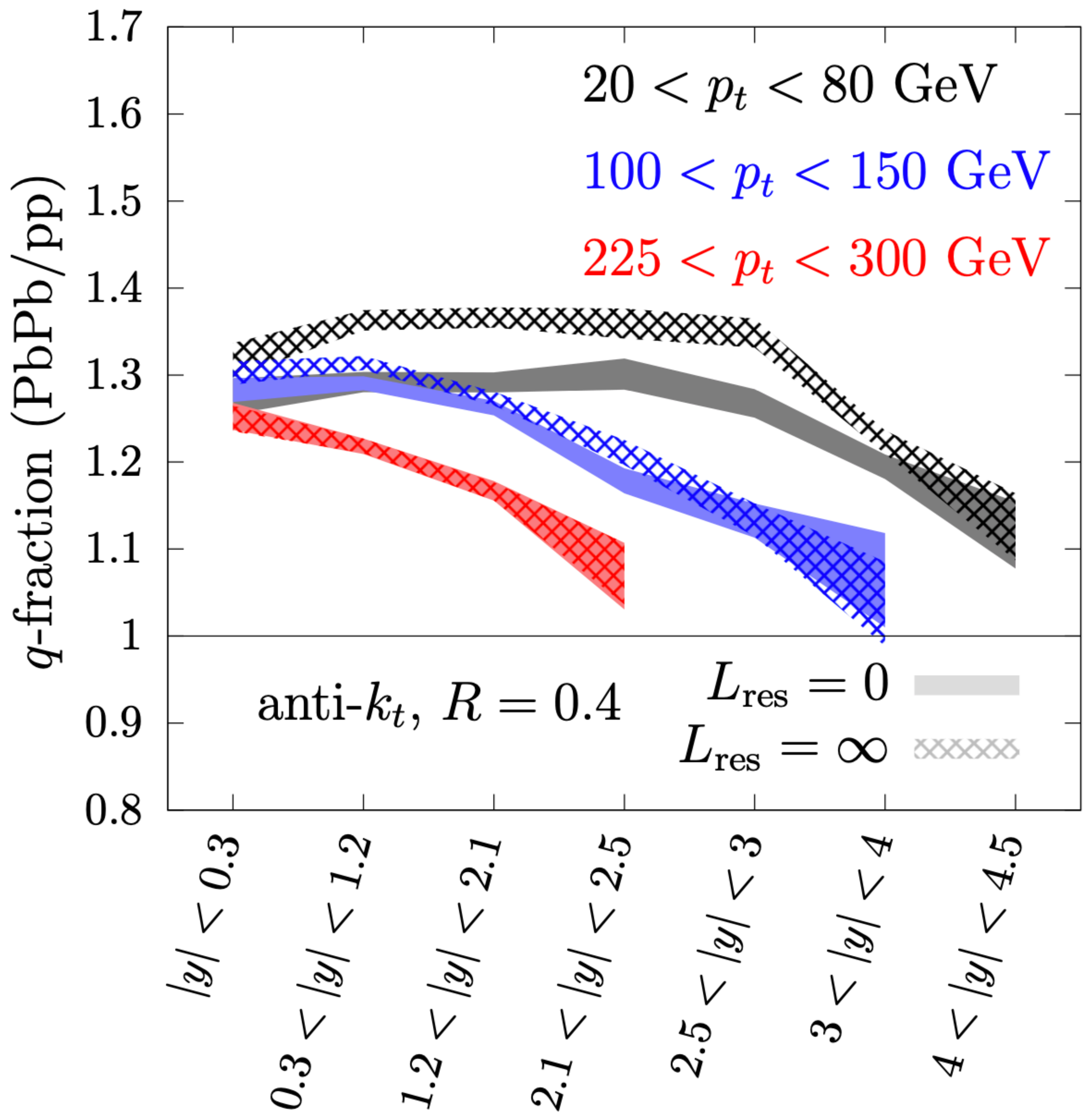

DP & A. Soto-Ontoso - 2210.07901

- At low p_T, q-fraction increases if sensitive to total color charge only.
  - → At high p_T, differences disappear.

- q-fraction ratio (PbPb/pp) in small e-loss approx:

$$f_q^{\text{ratio}} \approx 1 + (1 - f_q)(\varepsilon_g - \varepsilon_q)\frac{n}{p_t} + \mathcal{O}((\varepsilon n / p_t)^2)$$

Collimator in linearised approx:

Mehtar-Tani, Tywoniuk - PRD '18

$$\varepsilon_q \sim C_F \hat{\varepsilon}[1 + C_A \mathcal{A}(p_t, R)],$$
$$\varepsilon_g \sim C_A \hat{\varepsilon}[1 + C_A \mathcal{A}(p_t, R)]$$

$\mathcal{A}(p_t, R)$ is phase-space of extra energy loss sources.

$$\mathcal{A}_0 = \frac{\alpha_s}{\pi} \int \frac{\mathrm{d}z}{z} \int \frac{\mathrm{d}\theta}{\theta} \Theta(t_f < L)\Theta(\theta < R) = \frac{\alpha_s}{4\pi} \ln^2\left(\frac{p_t R^2 L}{2}\right),$$

$$\mathcal{A}_\infty \to 0$$

→ Explains behaviour in MC.

Hybrid Model

0-5% Centrality

Using statistics projected for HL-LHC

$k_t \equiv z(p_t^{\text{parent}}/p_t^{\text{jet}})\sin\theta/R$

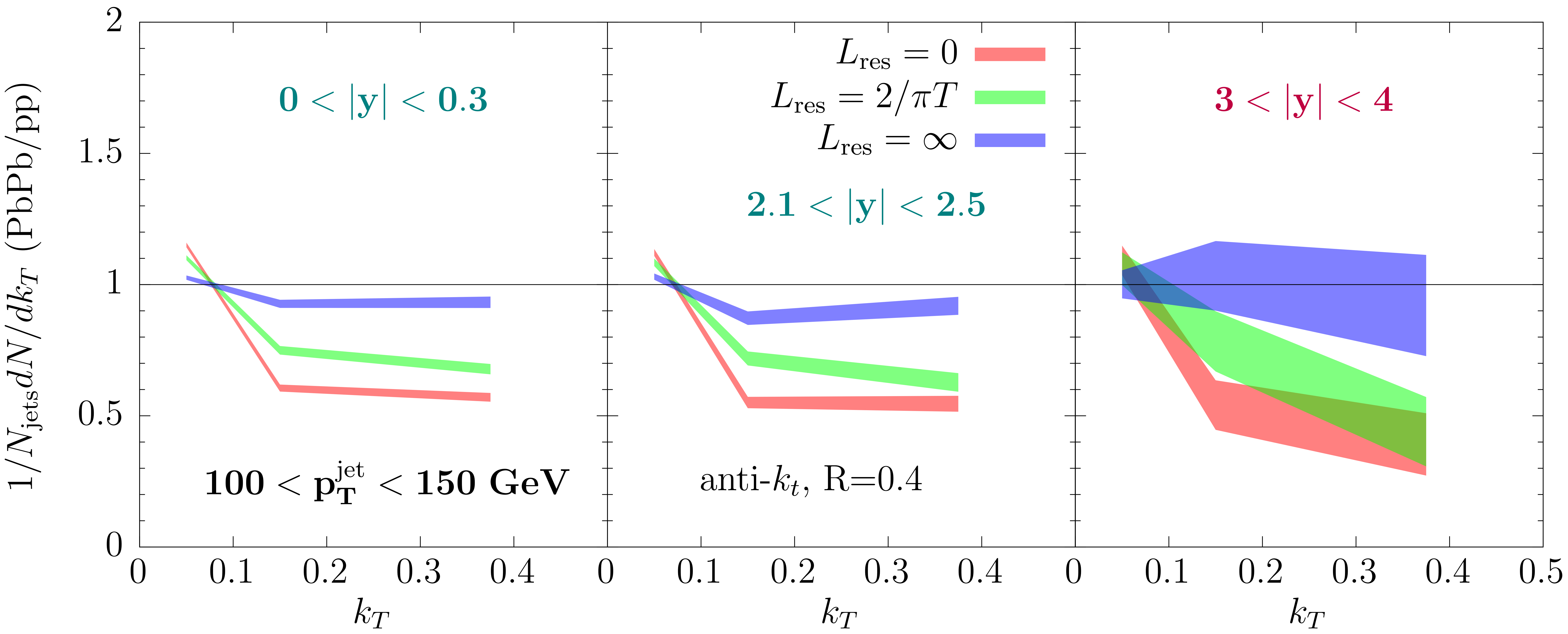

- Small effect from total charge quenching ($L_{res} = \infty$) at mid-rapidity.
- Narrowing persists at forward rapidities if jet substructure resolved (L_{res}=0 and L_{res}=2/πT).

DP & A. Soto-Ontoso - 2210.07901

Hybrid Model

0-5% Centrality

Using statistics projected for HL-LHC

$k_t \equiv z(p_t^{\text{parent}}/p_t^{\text{jet}}) \sin\theta/R$

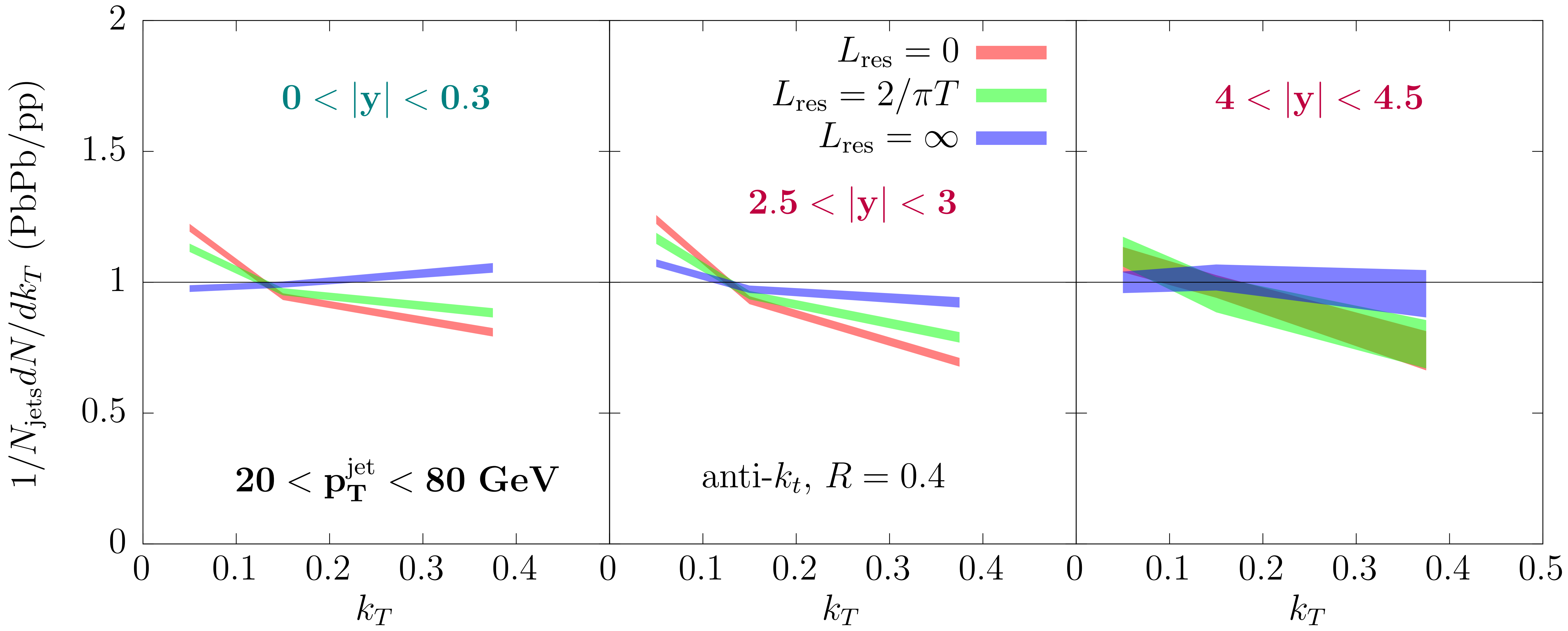

- Wake affects substructure of low p_T jets.
- At high rapidity, q-fraction evolves strongly with p_T.

→ Increasing rapidity can make distribution narrower due to jet p_T-bin migration.

DP & A. Soto-Ontoso - 2210.07901

Rapidity Evolution of Quark Fraction

DP & A. Soto-Ontoso - 2210.07901

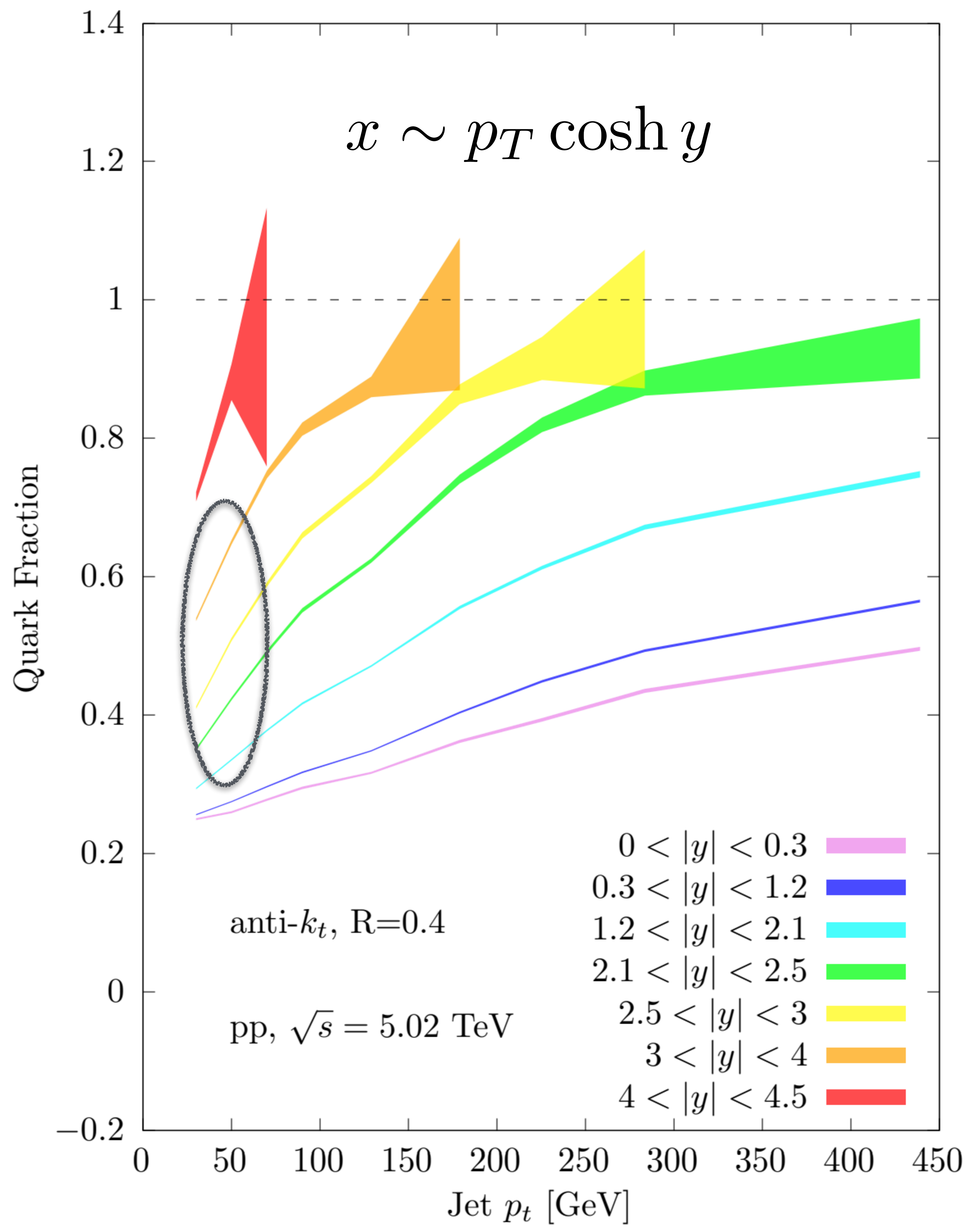

- Quark enriched samples can be obtained from e.g. inclusive b-tagged jets, semi-inclusive boson-jets.
- Here: exploit rapidity evolution of quark fraction to engineer quark enriched samples.

Extended rapidity coverages available in future detector upgrades.

ALICE3

Also ATLAS and CMS.

STAR

Forward Rapidity Upgrade
$2.5 < \eta < 4$

0-5% Centrality

Using statistics projected for HL-LHC

$$k_t \equiv z(p_t^{\text{parent}}/p_t^{\text{jet}}) \sin\theta/R$$

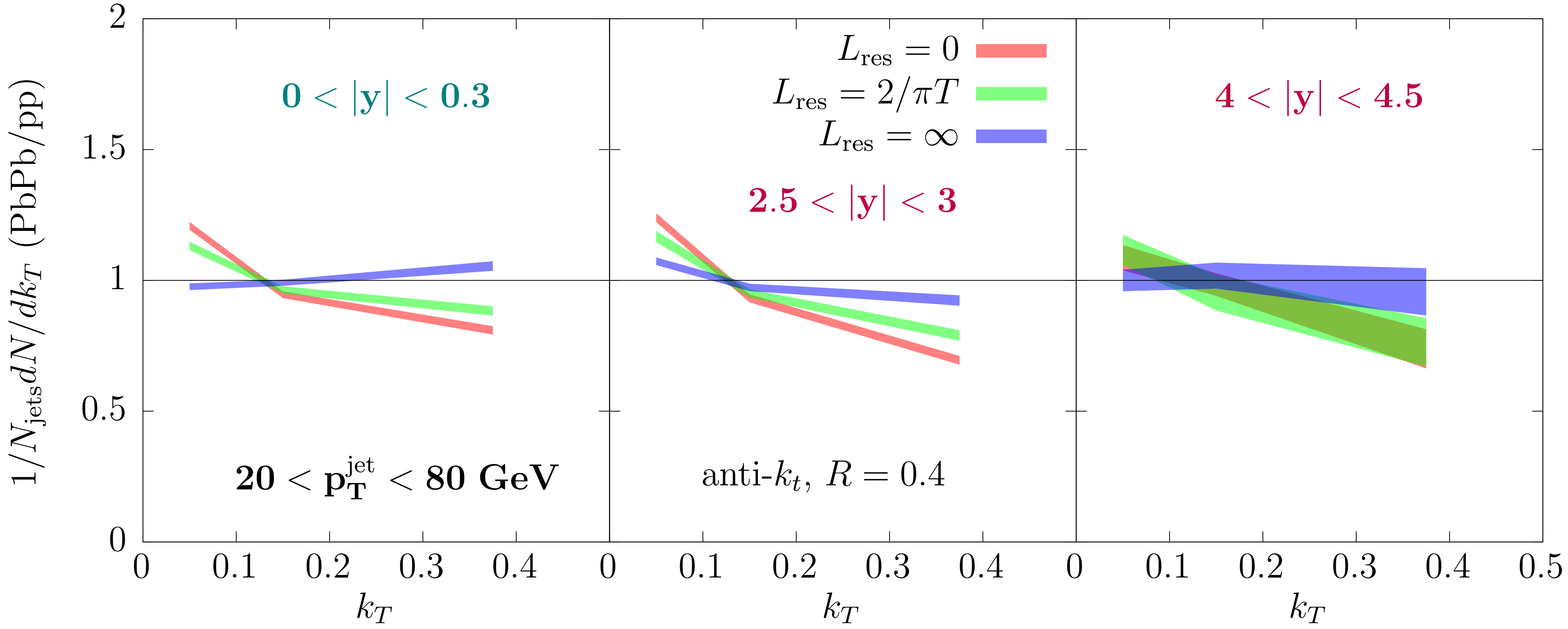

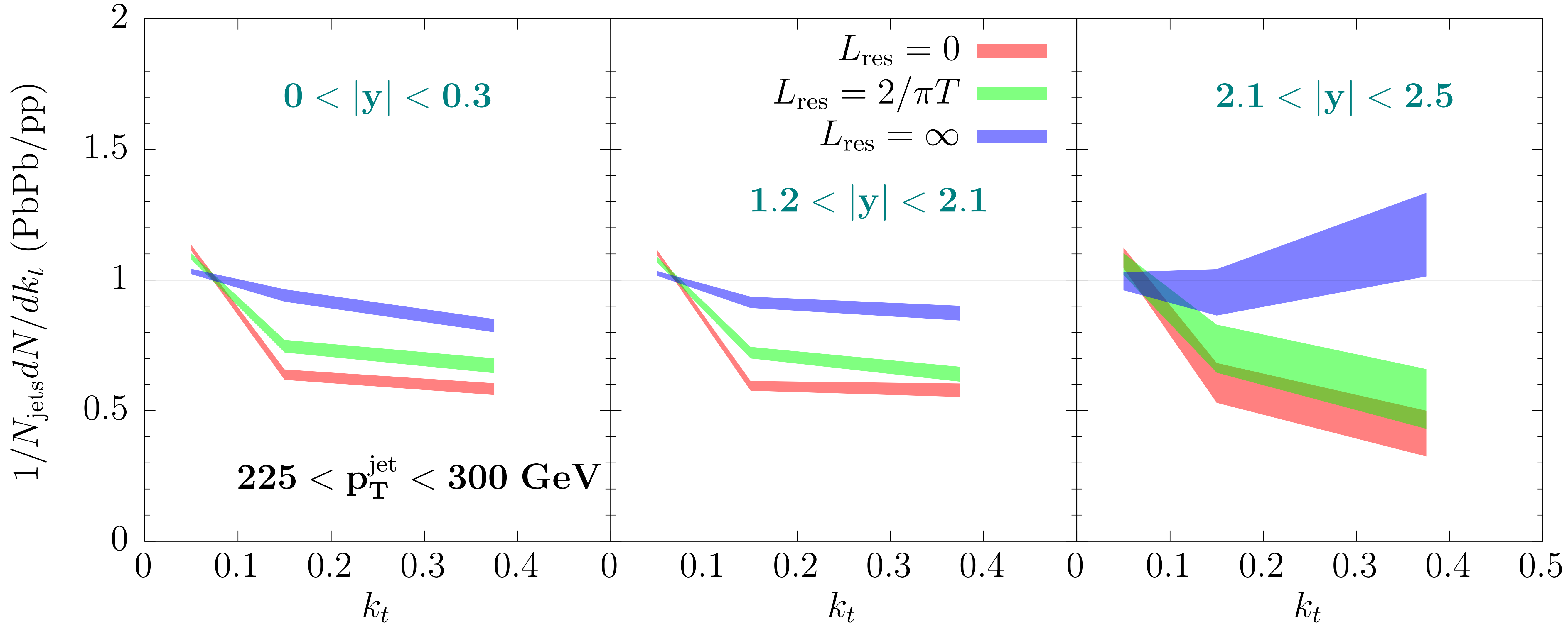

- Wake affects substructure of low p_T jets.
- At high rapidity, q-fraction evolves strongly with p_T.
  - → Increasing rapidity can make distribution narrower due to jet p_T-bin migration
- At high-enough p_T, current detectors' acceptance suffices to get high q-fraction.

DP & A. Soto-Ontoso - 2210.07901

Toy q/g Fraction Model

Using statistics projected for HL-LHC

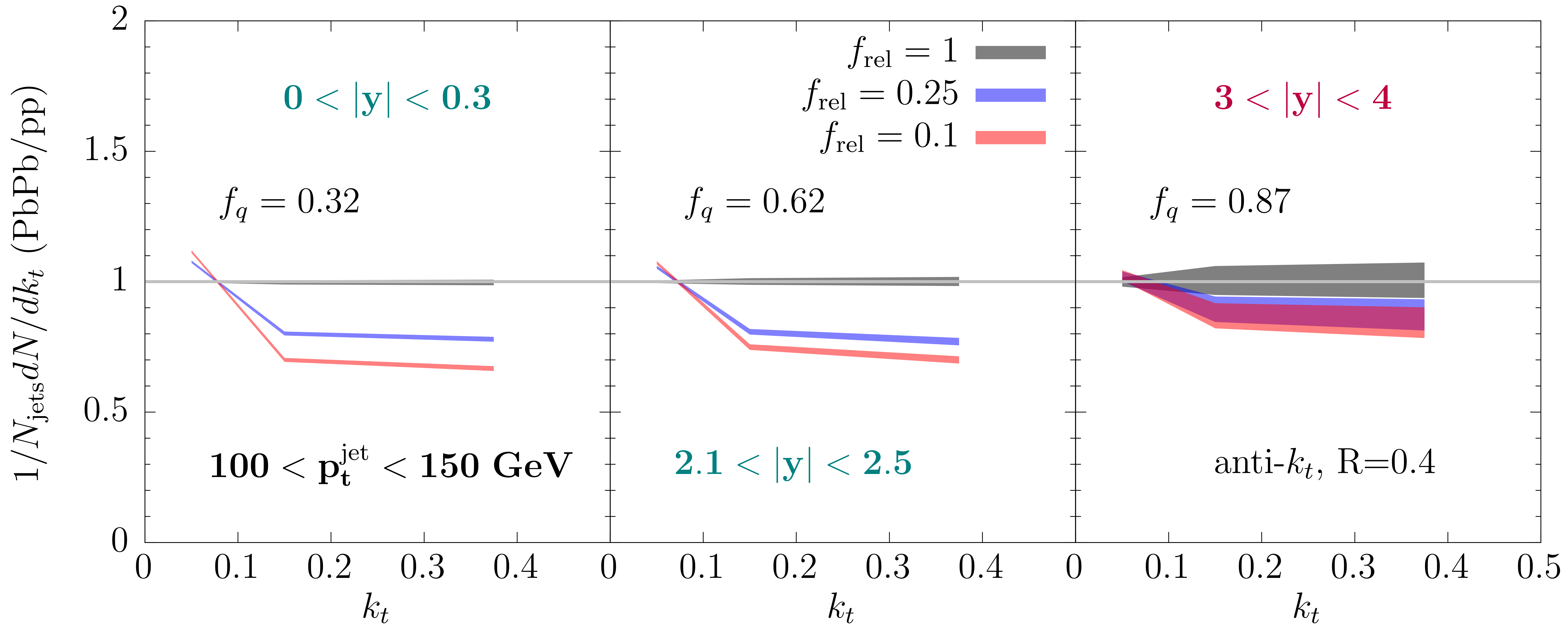

BDMPS-Z:

$$f_{rel} = \mathcal{Q}_q^{C_A/C_F - 1}$$

$$f_{rel} \approx 0.5$$

for $\mathcal{Q}_q = 0.6$

$$\frac{1}{\sigma}\frac{d\sigma}{dk_t}\Big|_{AA} = \mathcal{N}^{-1}\left[f_q \frac{d\sigma_q}{dk_t}\Big|_{pp} + f_{rel}(1 - f_q)\frac{d\sigma_g}{dk_t}\Big|_{pp}\right]$$

Combine quark and gluon pp templates with modified q/g fraction.

- Strong narrowing observed at mid-rapidity fades away toward forward rapidities.

DP & A. Soto-Ontoso - 2210.07901

Conclusions

- Jets possess a narrower substructure in heavy-ion compared to pp, due to selection bias.
  - → Wide versus narrow selection bias? **Medium** can **resolve** internal jet scales.
  - → Gluon versus quark selection bias? **Medium** does **not** need to **resolve** internal jet scales.

- Use quark enriched sample to disentangle physical picture. Exploit rapidity evolution of q-fraction.
  - → If there is still narrowing in quark enriched sample, then medium can resolve jet substructure.

Improved detector acceptance in HL-LHC era and STAR Forward Rapidity Upgrade

- Used leading-k_t distribution as proof-of-concept.
  - → No hard radiation or scatterings included. Baseline for future studies.
  - → Measurement at LHC shown at this conference.

Backup Slides

Jets in Vacuum

- Monte Carlo jet quenching models have provided crucial insights:

  → Naturally include multi-particle nature of jets.

  - DGLAP evolution

$$t\frac{\partial}{\partial t}f(x,t) \;=\; \int \frac{dz}{z}\frac{\alpha_s}{2\pi}P_+(z)\, f\left(\frac{x}{z},t\right)$$

use Sudakov form factor

$$\Delta_s(t) \;=\; \exp\left(-\int_x^{z_{max}} dz \int_{t_0}^{t}\frac{\alpha_s}{2\pi}\frac{dt'}{t'}\tilde{P}(z)\right)$$

  - Rewrite DGLAP as

$$f(x,t) \;=\; f(x,t_0)\Delta(t) + \int \frac{dt'}{t'}\frac{\Delta(t)}{\Delta(t')}\frac{\alpha_s(t')}{2\pi}\int\frac{dz}{z}P(z)f(\frac{x}{z},t')$$

Resums contributions to all orders in $\alpha_s \log t$

Sudakov: Poisson distribution with 0 mean: $P(0,p)=e^{-p}$ No (resolvable) emission

Convenient for MC sampling $P(1,p)=pe^{-p}$ One emission, etc…

Coherence in Vacuum: Heuristic Interpretation

Need to think in terms of the *formation time*

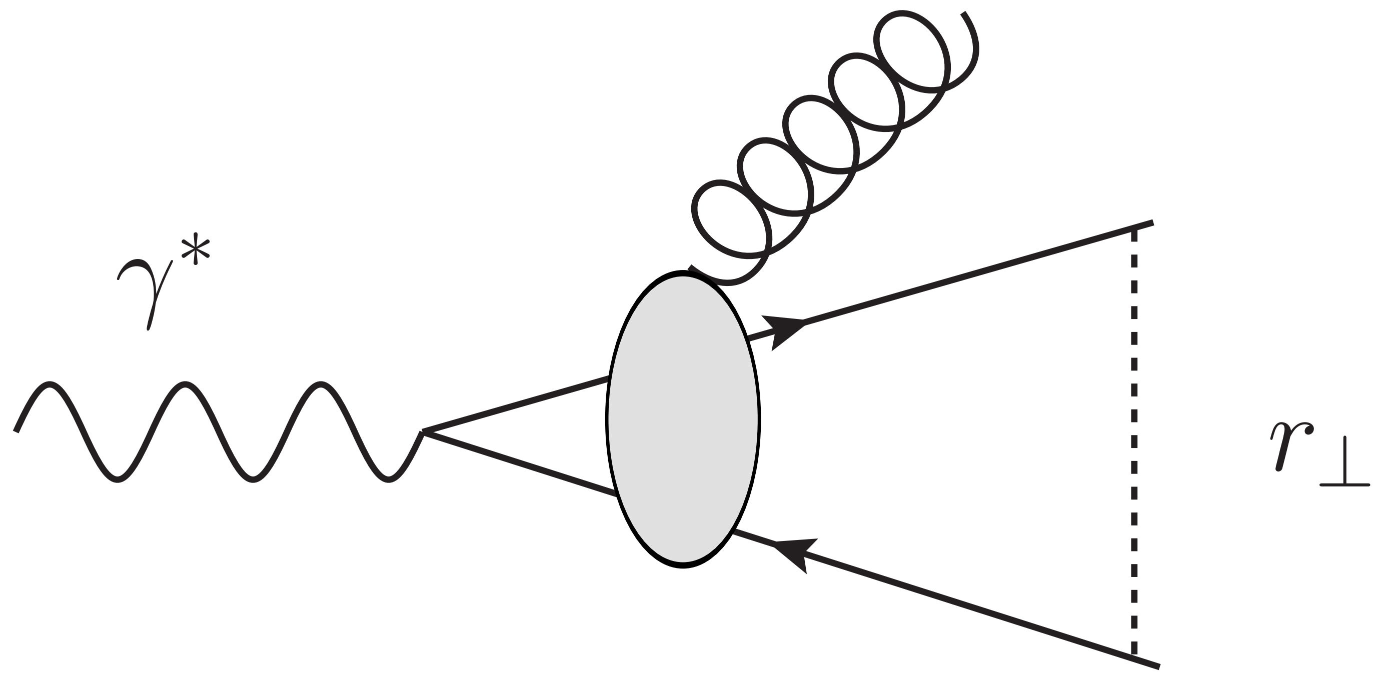

Time at which the gluon decorrelates from the quark:

$$\tau_f = \frac{w}{k_\perp^2} = \frac{1}{w\theta^2}$$

- Transverse size of the gluon is $\lambda_\perp \sim \frac{1}{k_\perp} = \frac{1}{w\theta}$
- Size of the antenna when the gluon is being emitted $r_\perp = \theta_{q\bar{q}}\tau_f = \frac{\theta_{q\bar{q}}}{w\theta^2}$

Compare the two:

→ If $r_\perp < \lambda_\perp$ the gluon cannot resolve the pair: coherent
No emission (color singlet) $\frac{r_\perp}{\lambda_\perp} < 1 \rightarrow \theta_{q\bar{q}} < \theta_q$

→ If $r_\perp > \lambda_\perp$ independent emission by quark and antiquark $\frac{r_\perp}{\lambda_\perp} > 1 \rightarrow \theta_{q\bar{q}} > \theta_q$

Radiative Energy Loss

- Framework: Light-Cone Perturbation Theory.
  - Integrated medium induced spectrum:

Baier, Dokshitzer, Mueller, Peigne, Schiff - NPB '97
Zakharov - JETP Lett. '96
Arnold, Moore, Yaffe - JHEP '03

$$\omega \frac{\mathrm{d}I}{\mathrm{d}\omega} = \frac{\alpha_s C_R}{\omega^2} \int_0^\infty dt_2 \int_0^{t_2} dt_1 \, \boldsymbol{\partial_x} \cdot \boldsymbol{\partial_y} \left[\mathcal{K}(\boldsymbol{x}, t_2 | \boldsymbol{y}, t_1) - \mathcal{K}_0(\boldsymbol{x}, t_2 | \boldsymbol{y}, t_1) \right]_{\boldsymbol{x}=\boldsymbol{y}=0}$$

- Resummed propagator due to multiple interactions with the medium satisfies 2D Schrödinger-like equation:

$$\left[i\partial_t + \frac{\boldsymbol{\partial}^2}{2\omega^2} + iv(\boldsymbol{x}) \right] \mathcal{K}(\boldsymbol{x}, t_2 | \boldsymbol{y}, t_1) = i\delta(\boldsymbol{x} - \boldsymbol{y})\delta(t_2 - t_1)$$

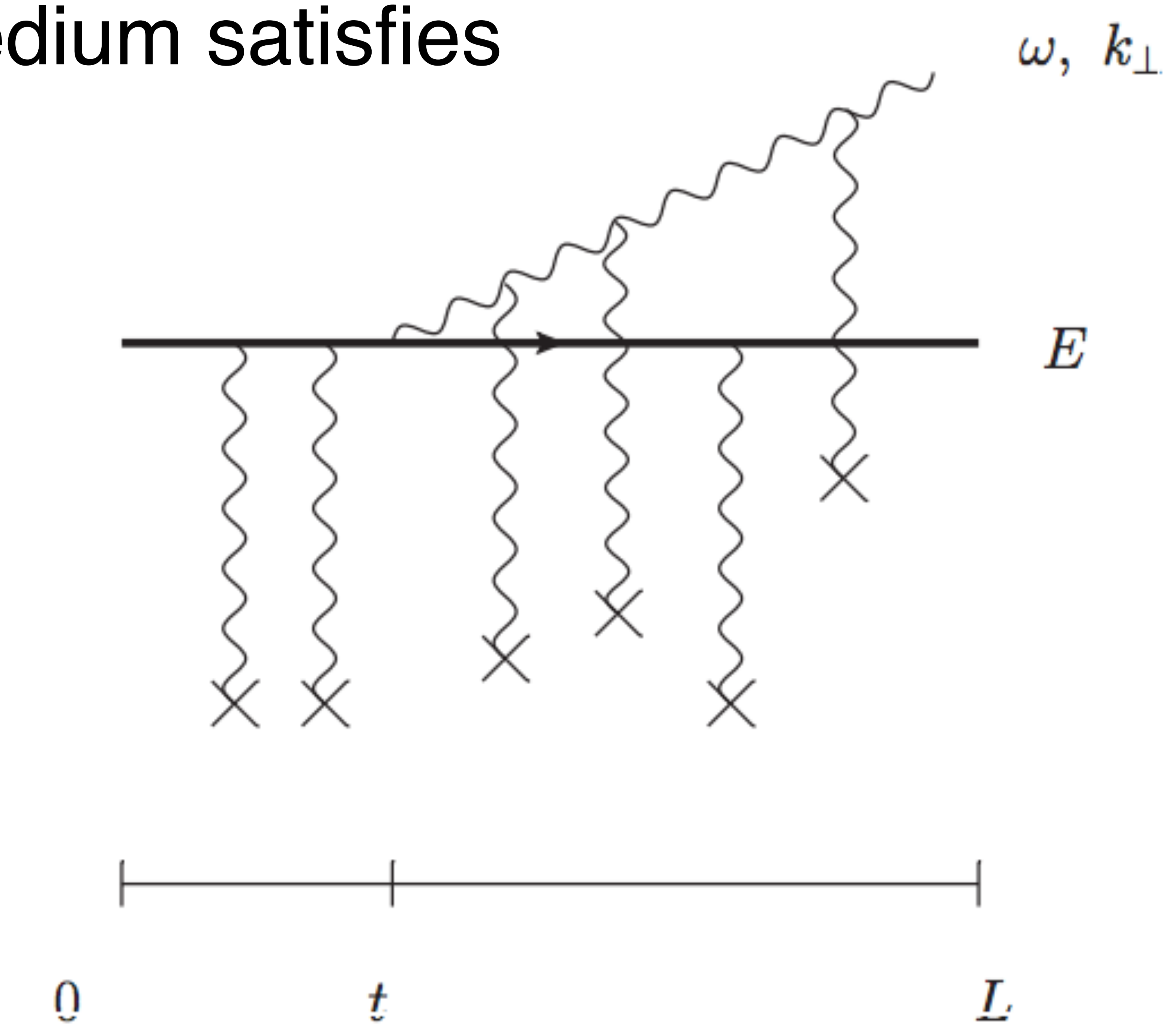

- With potential: $v(\boldsymbol{x}, t) = C_A \int_{\boldsymbol{k}} \frac{d^2\sigma}{d^2\boldsymbol{k}} (1 - e^{i\boldsymbol{k}\cdot\boldsymbol{x}})$

  and scattering cross-section:

Hard Thermal Loop:

$$\left(\frac{\mathrm{d}^2\sigma}{\mathrm{d}^2\boldsymbol{q}} \right)^{\mathrm{HTL}} = \frac{g^2 m_{\mathrm{D}}^2 T}{\boldsymbol{q}^2(\boldsymbol{q}^2 + m_{\mathrm{D}}^2)}$$

Gyulassy-Wang:

$$\left(\frac{\mathrm{d}^2\sigma}{\mathrm{d}^2\boldsymbol{q}} \right)^{\mathrm{GW}} = \frac{g^4 n(t)}{(\boldsymbol{q}^2 + \mu^2)^2}$$

Mehtar-Tani - JHEP '19

Usual Approximations of the Spectrum

- Dilute medium: expand to leading order in $v(\boldsymbol{x})$ (N=1 opacity expansion):

$$\omega\frac{\mathrm{d}I_{\mathrm{GLV}}}{\mathrm{d}\omega} = 32\pi\,\alpha_s\,C_R\,\hat{q}_0\int_0^L \mathrm{d}s\int_{\boldsymbol{p},\boldsymbol{q}}\frac{\boldsymbol{p}\cdot\boldsymbol{q}}{\boldsymbol{p}^2(\boldsymbol{p}-\boldsymbol{q})^2(\boldsymbol{q}^2+\mu^2)^2}\left\{1-\cos\left[\frac{(\boldsymbol{p}-\boldsymbol{q})^2}{2\omega}s\right]\right\}$$

Gyulassy-Levai-Vitev spectrum

Single hard scattering, preserves full form of potential.

Wiedemann - NPB ‘00
Gyulassy, Levai, Vitev - NPB ‘00
Wang, Guo - NPA ‘01
Majumder - PRD ‘12
Sievert, Vitev, Yoon - PLB ‘19

- Harmonic oscillator (diffusion) approximation:

$$v(\boldsymbol{x},t) = C_A\int_{\boldsymbol{k}}\frac{d^2\sigma}{d^2\boldsymbol{k}}(1-e^{i\boldsymbol{k}\cdot\boldsymbol{x}}) \equiv \frac{1}{4}\hat{q}(\boldsymbol{x}^2,t)\boldsymbol{x}^2 = \frac{1}{4}\hat{q}_0\boldsymbol{x}^2\log\left(\frac{1}{\mu^{\star 2}\boldsymbol{x}^2}\right)$$

neglect logarithmic dependence
$\mu^{*2}\sim 1/\mathbf{x}^2$

$$\omega\frac{\mathrm{d}I_{\mathrm{HO}}}{\mathrm{d}\omega} = 2\bar{\alpha}\ln|\cos(\Omega L)| \qquad \Omega(t) = \frac{1-i}{2}\sqrt{\frac{\hat{q}(t)}{\omega}}$$

BDMPS - ASW spectrum

Large medium, resums multiple soft interactions.

BDMPS-Z
Salgado, Wiedemann - PRD ‘03
Armesto, Salgado, Wiedemann - PRD ‘04

Null Falling Strings

npSYM

High energy partons in the QGP:

→ are dual to strings falling into a black hole, hydrodynamizing.

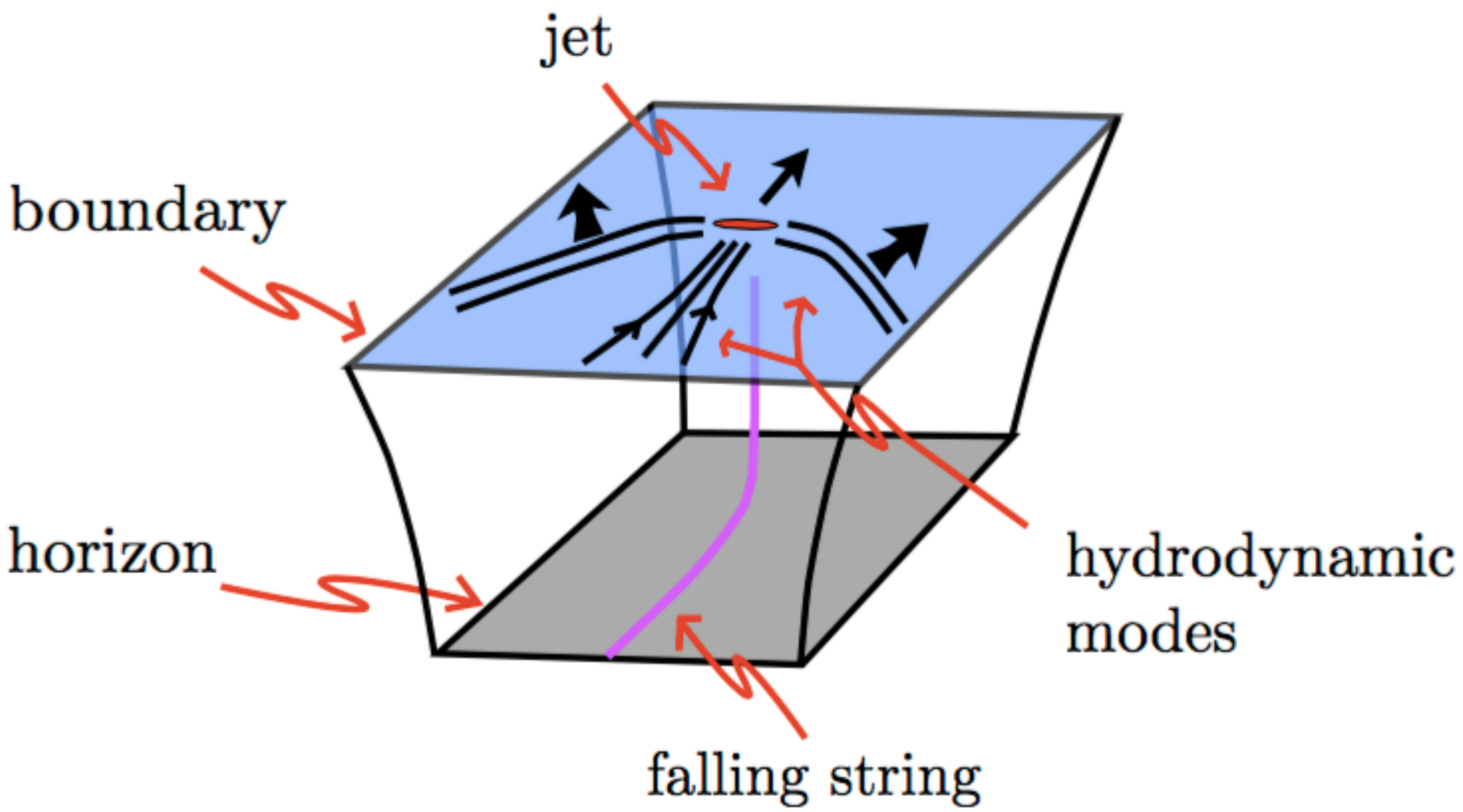

Chesler & Rajagopal - PRD ‘14, JHEP ‘16

$$\langle \Delta T^{\mu\nu}(t,\boldsymbol{x})\rangle = \frac{L^3}{4\pi G_{\rm Newton}} H^{(4)}_{\mu\nu}(t,\boldsymbol{x})$$

“Jet” induced EM tensor: hard + soft modes.

Perturbed metric @ boundary.

Long wavelength limit (hydrodynamization rate):

$$\frac{1}{E_{\rm init}}\frac{dE_{\rm jet}}{dx} = -\frac{4x^2}{\pi x^2_{\rm therm}\sqrt{x^2_{\rm therm}-x^2}}$$

The Wake of a Quark

- At strong coupling:
  - Modification of stress-energy tensor due to supersonic quark contains sound and diffusive modes.
  - Effective source for hydro corresponds to drag force on the quark.
  - Agreement between hydrodynamics & wake of a quark even for small distances ~ 1/T.

Energy flux

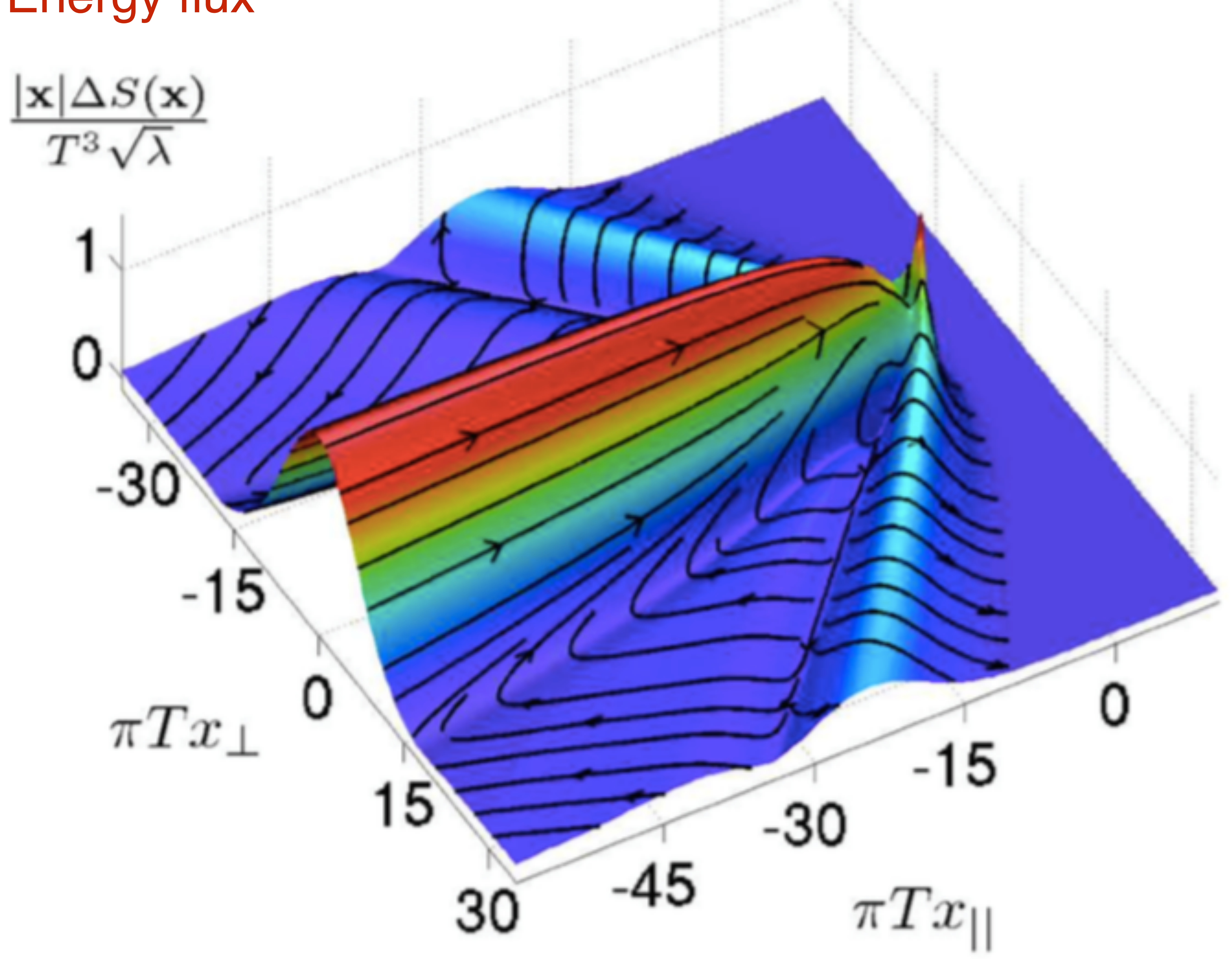

Fulfils Energy-Momentum Conservation in the Jet+Plasma Interplay.

Chesler & Yaffe - PRD '07

QGP Resolution Length

Take two extreme values for $L_{\rm res}$.

(explore realistic values later on)

- $L_{\rm res} = 0$ Fully resolved case.
- $L_{\rm res} = \infty$ Fully unresolved case.

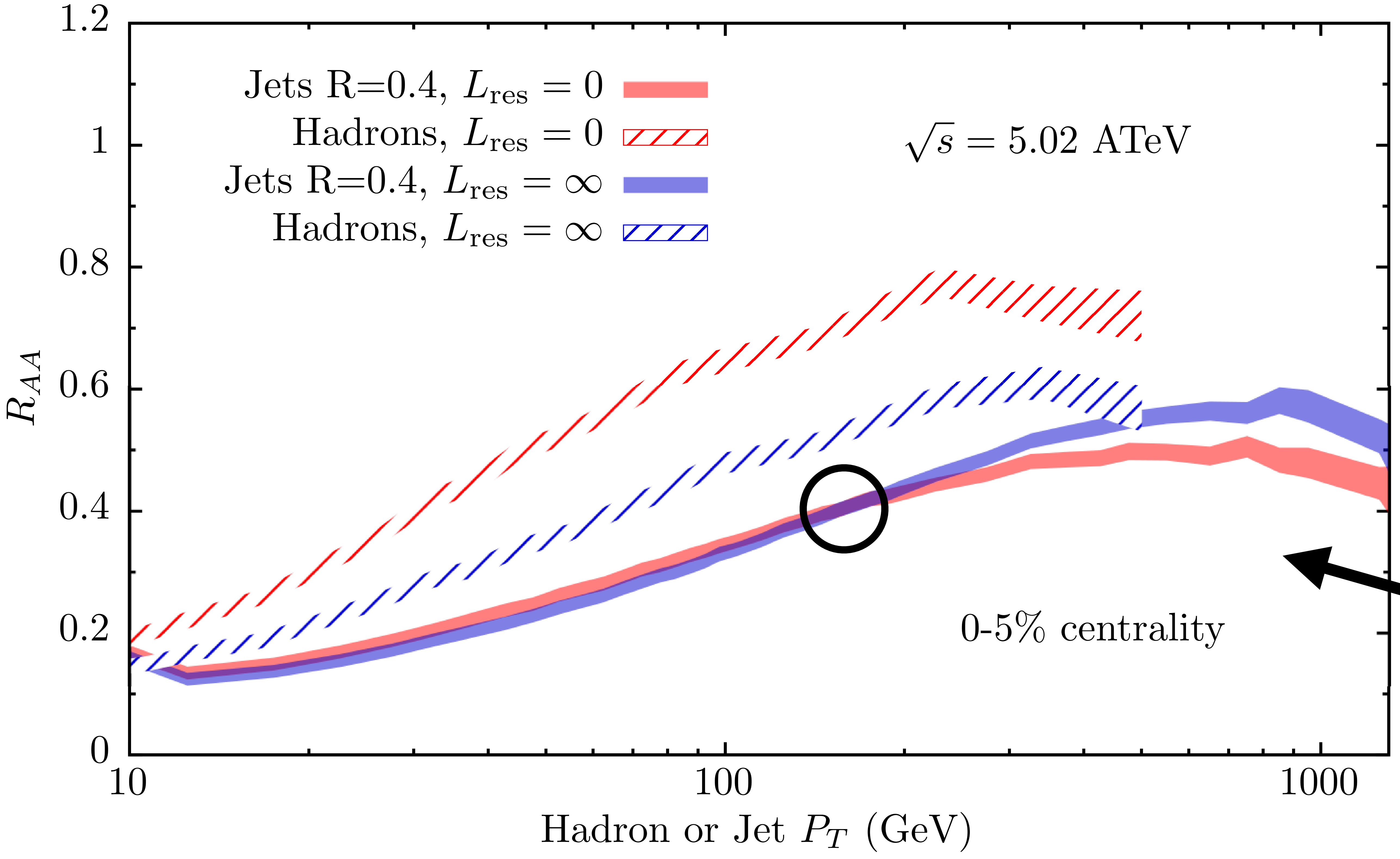

Amount of *jet* quenching depends on $L_{\rm res}$.

→ Adjust value of $\kappa_{\rm sc}$ to compare results at the same value of jet R_{AA}.

$L_{\rm res} = 0$: $0.404 < \kappa_{\rm sc} < 0.423$

$L_{\rm res} = \infty$: $0.5 < \kappa_{\rm sc} < 0.52$

Relative suppression of hadrons vs jets strongly depends on QGP resolution length.

(see Casalderrey-Solana, Hulcher, Milhano, DP, Rajagopal, PRC '19 and Mehtar-Tani & Tywoniuk, PRD '18)